

Mestrado Integrado em Engenharia Química

Studies in Displacement Ventilation Energy Efficiency and Thermal Comfort

Tese de Mestrado

desenvolvida no âmbito da disciplina de

Projecto de Desenvolvimento em Ambiente Empresarial

Tiago Filipe Marujo e Moreira

Fluidinova



Departamento de Engenharia Química

Orientador na FEUP: Professora Madalena Maria G. Q. Dias

Orientador na empresa: Engenheiro Manuel Filipe Ribeiro Madureira

July 2008

Acknowledgments

I would like to express my sincere gratitude to Filipe Madureira, my thesis advisor, for his unconditional support and guidance throughout this work. His encouragement along with his patience and suggestions gave me confidence and were determinant in the accomplishment of this work.

I would also like to thank Professora Madalena Dias and Professor José Carlos Lopes for their expertise and counseling during this work; their suggestions were crucial during this project.

I must also thank Paulo Gomes for introducing me to the CFD world. His support in this area, as well as his confidence and promptness were very important during this work.

I am grateful to Joana Cardoso and Claudio Fonte for their time and knowledgeable help in the ES field, and to Pedro Afonso and Carlos Fonte for their help with the CFD software.

I would like to thank my friend Rui Faria, also a master student at Fluidinova, for the support during this five months.

My sincere thanks must be extended to all the colleagues and friends at Fluidinova for making it such a great place to be a part of.

A special thank you for my family for their encouragement, support and endless love.

Finally, I wish to thank my girlfriend, Ana, for her patient, understanding and unconditional support.

To my Parents

For their never-ending love and support through life

Abstract

The present work aims to study the performance and relevance of Displacement Ventilation in buildings. Two cases were studied using EnergyPlus: a simple model building and an existing office tower in Lisbon. Special emphasis was given to the evaluation of Thermal Comfort and Energy Efficiency.

Various configurations were studied, in order to obtain the best operating conditions on both buildings. Whenever possible the results were compared to an equivalent mixing ventilation system in order to infer the improvement or decline of the operative conditions

EnergyPlus is a certified software in the Energy Simulation area, but it lacks validation in the incorporated Displacement Ventilation models. It is also the aim of this work to validate the results obtained by comparing the Energy Plus predictions with the results obtained with the Computational Fluid Dynamics simulations.

Keywords:

Displacement Ventilation; Energy Simulation; EnergyPlus; CFD; Thermal Comfort; Energy Efficiency.

Resumo

O presente trabalho pretende estudar o desempenho e as vantagens da ventilação por deslocamento em edifícios. Foi utilizado o software EnergyPlus para estudar o modelo de um edifício simples e numa outra fase, um edifício de escritórios localizado em Lisboa. Neste estudo deu-se especial atenção à eficiência energética e ao conforto térmico.

Foram estudados todos os parâmetros do modelo, no sentido de se obterem as melhores condições de operação nos dois edifícios. Sempre que possível, os resultados do modelo de ventilação por deslocamento foram comparados com um modelo de ventilação por mistura equivalente.

O Energy Plus é um software certificado na área de simulação energética, mas carece de validação dos modelos de ventilação por deslocamento nele existentes. Desta forma é também objectivo desta tese validar os resultados obtidos na simulação energética, comparando-os com os resultados obtidos por Computação de Fluídos Dinâmicos.

Palavras chave:

Ventilação por Deslocamento; Simulação dinâmica energética; EnergyPlus; CFD; Conforto térmico; Eficiência energética.

Table of Contents

Table of Contents	i
List of Figures.....	iii
List of Tables.....	vi
Nomenclature.....	vii
1 Introduction	1
1.1 Motivation and Relevance.....	1
1.2 Thesis Objectives and Layout	2
2 State of the art.....	3
2.1 Mixing Ventilation	3
2.2 Displacement Ventilation	4
2.3 Energy Simulation Software	7
2.3.1 Displacement ventilation models.....	8
2.3.2 Variable Air Volume Fan System.....	10
2.3.3 Thermal Comfort.....	11
2.4 Computational Fluid Dynamics.....	12
3 Technical Description and Results	14
3.1 Model Description.....	14
3.2 Simple Model Building.....	16
3.2.1 Model Building Description	16
3.2.2 Parametric Study.....	20
3.2.3 EnergyPlus Simulation Results	25
3.3 Validation of EnergyPlus Model with CFD.....	29
3.3.1 ES Model Description	29
3.3.2 CFD Model Description	29
3.3.3 EnergyPlus versus Fluent Simulation Results	31
3.4 Real Building Model.....	36
3.4.1 Model Description.....	37

3.4.2	Energy Simulation Results	40
4	Conclusion	45
5	Final Remarks	46
5.1	Accomplished goals	46
5.2	Future Work	46
5.3	Final Appreciations	47
6	References	49
Appendix A.	Detailed RSECE Information	i
Appendix B.	Detailed Information about Building X	i
B.1	Profiles of occupation, lighting system and equipment.....	i
B.2	Constructive Solutions of Building X:	ii

List of Figures

Figure 1 - Typical airflow in a room with a mixing ventilation system (adapted from (Butler, 2002)). 3

Figure 2 - Illustration of the airflow pattern in Displacement Ventilation (adapted from Skistad) .. 4

Figure 3 - Vertical temperature distributions for mixing and displacement ventilation (Mundt, Skistad, Nielsen, Hagstrom, & Railio, 2004). 5

Figure 4 - Short circuit motivated by the supply of warm air ((Mundt, Skistad, Nielsen, Hagstrom, & Railio, 2004)). 5

Figure 5 - Air contaminants airflow, in DV system (Mundt, Skistad, Nielsen, Hagstrom, & Railio, 2004) 6

Figure 6 - Variable Air Volume system diagram 10

Figure 7 - Predicted mean vote (PMV) comfort scale 12

Figure 8 - Illustrative image of the model building..... 16

Figure 9 - Monthly maximum, minimum and mean temperatures. 17

Figure 10 - Monthly time distribution of a given relative humidity...... 17

Figure 11 - Total monthly evolution solar radiation, both diffuse and direct..... 18

Figure 12 - Monthly evolution of wind speed (a) and direction (b)..... 18

Figure 13 - Transition height, for three thermostat heights, during a winter day (b) and a summer day (b). 20

Figure 14 -Percentage time of comfort for the three thermostat heights..... 21

Figure 15 - Energy consumption for cooling for the three studied thermostat positions..... 21

Figure 16 - Energy consumption for cooling for the three studied GD fractions 22

Figure 17 -Charts with the transition height, for the three different GD, during a winter day (a) and during a summer day (b) 22

Figure 18 -Charts with the Inflow rate, for the three different GD, during a winter day (a) and during a summer day (b) 23

Figure 19 - Energy consumption for cooling for the three studied heat gains..... 23

Figure 20 - Charts with the transition height, for the three different heat gains, during a winter day (a) and a summer day (b)..... 24

Figure 21 - Charts with the inflow rate, for the three different heat gains, during a winter day (a) and a summer day (b) 24

Figure 22 - Zone temperatures during a representative winter day for MV and DV systems...... 25

Figure 23 -Zone temperatures during a representative summer day for MV and DV systems...... 26

Figure 24 - Variation of the conditioning volume during a typical winter day a) and a summer day b) 26

Figure 25 - Inlet volume flow rate during a typical winter day a) and summer day (b). 27

Figure 26 - Monthly heating energy consumption for DV and MV systems..... 27

Figure 27 - Monthly cooling energy consumption for DV and MV systems 27

Figure 28 - Annual energy consumptions for heating, cooling and ventilation 28

Figure 29 - Histogram with comfort time percentage for both systems..... 28

Figure 30 - Image of the building finite element grid 30

Figure 31 - Temperature contours across the x-axis. 32

Figure 32 - Temperature contours across the y-axis 32

Figure 33 - Iso-temperature surface at 24°C..... 33

Figure 34 - Height distribution of the iso-temperature surface of Figure 33..... 33

Figure 35 - Streamlines with temperature contours. 34

Figure 36 - Detail of the streamlines with temperature contours from the supply inlet grid. 34

Figure 37 - Height versus temperature for two different y values on plane $x = 8.55\text{m}$ (see Figure 38)..... 35

Figure 38 - Temperature contours across the x-axis for $x = 8.55\text{m}$ 35

Figure 39 - Temperature profiles inside the room 36

Figure 40 - Images of the model designed using DB and EP. a) Building detail. B) Shadowing effect of building surrounding 37

Figure 41 - Images of a) the existent building and b) the model used on EP 37

Figure 42 - Monthly maximum, minimum and mean temperatures 38

Figure 43 - Monthly time distribution for a given relative humidity..... 38

Figure 44 - Monthly evolution of wind speed (a) and direction (b)..... 38

Figure 45 - Total monthly evolution of solar radiation, both diffuse and direct 39

Figure 46 - Induction unit during a) heating and b) cooling operation 39

Figure 47 - Thermal energy spent with the current HVAC system, during a typical winter period a) and a typical summer period b) 40

Figure 48 - Thermal energy spent with DV system, during a typical winter period a) and a typical summer period b)..... 41

Figure 49 - Monthly energy consumption, for cooling (a) and heating (b), during the year..... 41

Figure 50 - Summary of the energy spent on both systems 42

Figure 51 - Predicted mean vote for both systems studied 43

List of Tables

Table 1 - Table with the thermal properties of the floor materials 16

Table 2 - Table with the thermal properties of the ceiling materials 17

Table 3 - Table with the thermal properties of the wall materials 17

Table 4 - Densities of occupation, equipment and lighting system predicted by RSECE 19

Table 5 - Parameters used on the UCSD-DV model 25

Table 6 - Simulation conditions for displacement and mixing ventilation 25

Table 7 -EP tuned weather file conditions 29

Table 8 - Physical Models Used 30

Table 9 - Boundary Conditions used to run the simulation 31

Table 10 - Summary results from EP and CFD simulations. 36

Table 11 - General densities of occupation, lighting system and equipment 39

Table 12 - Simulation Conditions for the mixing and displacement ventilation systems 40

Nomenclature

ρ	Air Density	kg/m ³
A	Area	m ²
B	Buoyancy flux	m ⁴ /s ³
C_P	Thermal Capacity (Constant Pressure)	J/kg/°C
g	Gravitational acceleration	m/s ²
G_{FR}	Gain distribution fraction	-
h_c	Convective heat transfer coefficient	W/m ² /°C
h	Transition height	m
k	Thermal conductivity	W/m/°C
\dot{m}	Mass flow	kg/s
N_{Plumes}	Number of plumes	-
\dot{Q}	Amount of heat	W
\dot{Q}_{Plumes}	Heat removed by the plumes	W
\dot{Q}_{sys}	Heat removed by the system	W
$\dot{Q}_{OccZone}$	Heat gains of the occupied zone	W
\dot{Q}_{MxZone}	Heat gains of the mixed zone	W
$\dot{Q}_{PerPlume}$	Heat remove per plume	W
R_i	Thermal Resistance	K m ² /W
T	Temperature	°C
T_{sup}	Air Supply Temperature	°C
T_{exh}	Air Exhaust Temperature	°C
T_{mx}	Temperature of the mixed zone	°C
T_{occ}	Temperature of the occupied zone	°C
T_{Floor}	Temperature of the floor zone	°C
U	Global heat Transfer Coefficient	W/m ² /K
\dot{V}	Volume Flow rate	m ³ /s

Lista de Siglas

CFD	Computational Fluid Dynamics
CV	Constant Air Volume
DV	Displacement Ventilation
DVRA	Displacement Ventilation Room Air
EP	EnergyPlus
ES	Energy Simulation
GD	Gain Distribution
HVAC	Heating Ventilation and Air Conditioning
MV	Mixing Ventilation
PMV	Predicted Mean Vote
RSECE	Regulamento dos Sistemas Energéticos e de Climatização nos Edifícios
TC	Thermal Comfort
TH	Thermostat Height
UCSD	University of California, San Diego
UFAD	Under Floor Air Distribution
VAV	Variable Air Volume

1 Introduction

1.1 Motivation and Relevance

Currently, most buildings use mixing ventilation systems to conditioning the indoor air temperature and humidity, which may not be the most efficient solution.

In the last few years the demand for energy efficiency influenced various areas, including building ventilation. As a consequence there was an increased research on naturally driven ventilation systems, such as Natural Ventilation, Cross Ventilation and Displacement Ventilation.

The design of this sort of systems soon became a problem, because they were, mostly, planned using simple rules-of-thumb. The alternative was to use Computational Fluid Dynamics (CFD) but this was limited by the high computational power required. EnergyPlus (EP) is the latest energy simulation software, it was developed by the Department of Energy of the USA, and has lower computational requirements, but it was designed only to simulate Mixing Ventilation Systems. Energy Simulation (ES) allows studying the performance of a building along time, in a dynamic way, considering the hourly weather data and building activity. Recently, some authors adapted their models to run in EnergyPlus, enabling the capacity to simulate numerous systems based on naturally driven ventilation systems. This change was quite challenging, since EP does not model the airflow inside the room. The air behavior is modeled using correlations and approximations. These models, after their integration in EP, are relatively easy to use and require much less computational power than the CFD software. However, all software needs to be validated, and while CFD has demonstrated good results for the mixing and naturally driven ventilation, EP has been only validated for mixing ventilation systems.

Fluidinova, Engenharia de Fluidos, S.A. is a high technology engineering company. One of its core business areas is the consulting service in industrial processes, buildings and environment, using Computational Fluid Dynamics and Energy Simulation Software - CFDapi

Consulting projects for industrial processes, result in not just the detection of problems, but also provide re-engineering solutions and development of new fluid circulation equipment. Consulting service for building energy simulation can reduce the design time and promote the development of sustainable buildings, while increasing the architect and designer team creativity.

The search of new and more efficient technologies is the aim of this company. With this work, Fluidinova will be able to study the implementation of displacement ventilation systems in future buildings, contributing for a better, more efficient, sustainable world.

1.2 Thesis Objectives and Layout

This work has two main objectives:

1. To compare the predicted results obtained in Energy Plus with CFD simulation results for displacement ventilation systems, using a simple model building.
2. To study the performance of displacement ventilation systems in comparison with mixing ventilation systems in a real building, using Energy Plus. The performance of the building will be evaluated according to the energy savings and thermal comfort.

This thesis is divided into five chapters:

This first chapter, Chapter 1, briefly introduces the studies developed in this thesis.

In Chapter 2, the current know-how in displacement ventilation is reviewed, and the mechanism is described in detail. The tools used to accomplish the studies in this work are also described in this chapter.

Chapter 3 describes the major studies and tasks performed. The most important results are presented and explained in this part. First a simple model building was created and studied. Predictions of the ES are compared to CFD simulation results, in order to validate the EP tool used. Then an existing office building was studied where a DV system is compared to the existent MV system. Energy consumptions during the heating and cooling seasons are compared, as well as the comfort of the occupants inside the building.

The general conclusions of this work are listed on the fourth chapter, while the evaluation of the work along with suggestions for future work, can be found in Chapter 5.

2 State of the art

Usually people stay about 80-90% of their time inside buildings, where they are supposed to feel comfortable, healthy and at the same time, work and do other chores as efficiently as possible. In many cases these buildings are designed with inefficient climate control systems, and consume large amounts of energy to guarantee the correct temperature and humidity. Present concerns with energy efficiency coupled with the imposed high standards of performance contemporary building industry make this situation unacceptable.

Buildings are conditioned, mostly, with one of three types of ventilation: Mixing Ventilation (MV), Displacement Ventilation (DV) and Natural Ventilation.

2.1 Mixing Ventilation

Mixing ventilation has been the most popular method for air distribution since the advent of mechanical ventilation. The air is supplied and exhausted from the room at high velocities to induce mixing (Figure 1). The diffusers have to be designed so that the fresh air has enough time to entrain the warmer room air before directly impacting people. The high velocities of the air streams result in momentum diffusion leading to the absence of a preferred direction for air motion in the room. Such condition helps to maintain an even temperature distribution, but as a consequence it also distributes the contaminants produced by the heat sources present in the room (Arens, 2000). The dilution of the contaminants may reduce the Indoor Air Quality (IAQ) inside a room (Mundt, Skistad, Nielsen, Hagstrom, & Railio, 2004).

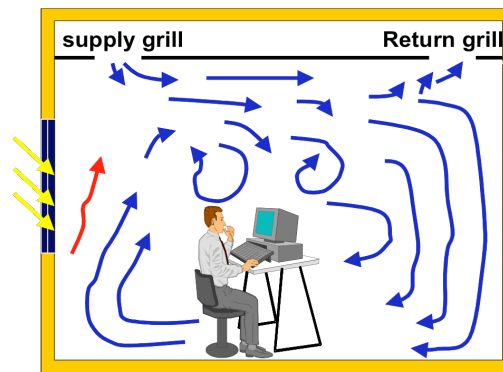


Figure 1 - Typical airflow in a room with a mixing ventilation system (adapted from (Butler, 2002)).

Normally, MV is well suited for both heating and cooling with no need of a secondary heating system. The total amount of energy removed from a room by the ventilation system is given by

$$Q_{total} = \rho C_p \dot{V} (T_{exh} - T_{sup}) \quad (1)$$

where Q_{total} is the total heat removed from the room, in W, \dot{V} is the room ventilation rate in m^3/s , ρ is the air density in kg/m^3 , C_p is the air specific heat capacity at constant pressure in $J/kg/^\circ C$, T_{exh} and T_{Sup} are, respectively the exhaust and inlet air temperatures in $^\circ C$.

2.2 Displacement Ventilation

Displacement Ventilation (DV) systems were first introduced in the Scandinavian countries during the 1970s (Mundt, Skistad, Nielsen, Hagstrom, & Railio, 2004). These systems take advantage of the thermal stratification that is formed inside a room. In fact the basis of DV is very simple, the supply air that flows across the floor, is warmed by the heat sources, producing buoyant plumes that will force the air to move vertically to the top of the room, where it will be exhausted. Whenever the room internal gains occur predominantly in the form of plumes, a noticeable interface occurs between the occupied zone and the mixed warmer zone, near the ceiling. To minimize mixing of the warmer layer with the occupied zone, low inlet velocities are required. There are many studies showing this clear transition between the two zones (Butler, 2002; Graça, 2003; Fitzgerald & Woods, 2007; Száday). Figure 2 illustrates the described mechanism.

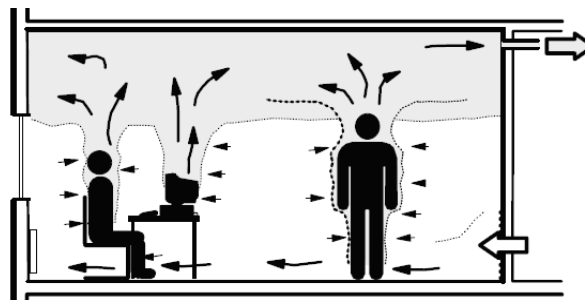


Figure 2 - Illustration of the airflow pattern in Displacement Ventilation (adapted from Skistad)

The supply air temperature is usually higher than in MV systems and the inlet velocities are smaller to prevent discomfort by cold draft. This might limit the maximum inflow in a certain room, and therefore limit the heat removal from the occupied zone. The advantage of the higher inlet temperatures (typically near 20-22 $^\circ C$ against the 15-16 $^\circ C$ in MV) is the extension of the free cooling time. This means that when the outside air temperature is below the 20-22 $^\circ C$ it is possible to use more outside air than the minimum required to ensure acceptable IAQ and to reduce the occupied zone temperature instead of recycling indoor room air (Butler, 2002).

The main temperature gradient is vertical and the air velocities are small in the entire room. Usually for rooms higher than 3 m, the temperature difference between the air near the floor and the air near the ceiling is about 4 $^\circ C$. This is a great advantage of DV, since it will only condition the occupied zone air temperature and relative humidity, instead of

conditioning the whole room volume, resulting in a drastically reduction of energy consumption. Figure 3 shows the temperature gradients for typical DV and MV systems as well as their typical inlet temperatures.

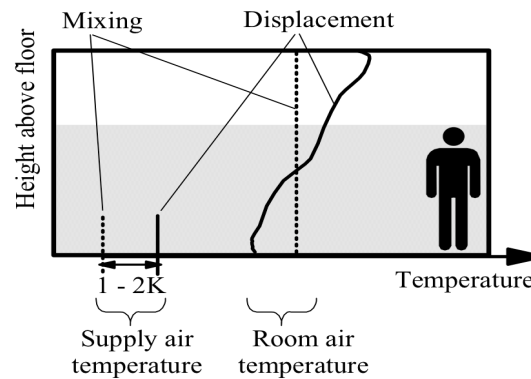


Figure 3 - Vertical temperature distributions for mixing and displacement ventilation (Mundt, Skistad, Nielsen, Hagstrom, & Railio, 2004).

Rooms ventilated by DV should not be heated by ventilation air because the warm air will rise to the top of the room due to buoyancy, resulting in a short circuit, leading the air to leave the room almost unaffected, as illustrated in Figure 4. Additionally, if the room envelope is colder than the occupied zone, the descending wall boundary layer flow may disrupt the stratification, bringing the warmer air from the upper layer to the occupied zone (Mundt, Skistad, Nielsen, Hagstrom, & Railio, 2004).

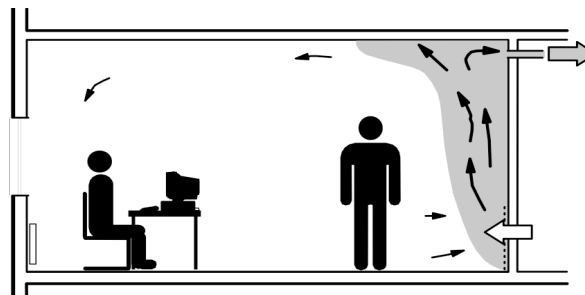


Figure 4 - Short circuit motivated by the supply of warm air (Mundt, Skistad, Nielsen, Hagstrom, & Railio, 2004).

The performance of a DV system depends on many conditions but, generally, if a vertical stratified temperature gradient can be established, then the air quality can be improved and the energy consumption can be reduced.

Although both MV and DV require about the same airflow, DV generally gives a better air quality for the same amount of ventilation air. The low velocities of the air reduce mixing, improving the air quality since air pollutants will be dragged out of the occupied zone into the upper mixed zone, as shown in Figure 5.

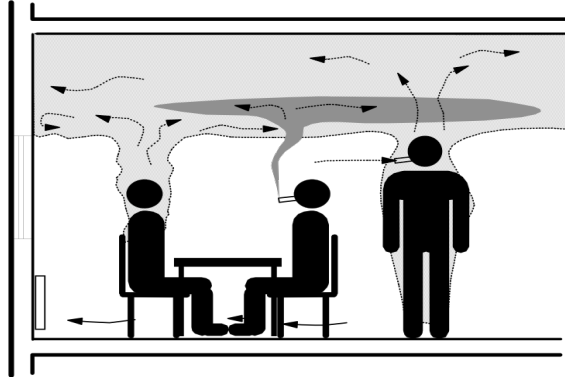


Figure 5 - Air contaminants airflow, in DV system (Mundt, Skistad, Nielsen, Hagstrom, & Railio, 2004)

Displacement ventilation is an efficient ventilation technique with a great potential. The vertical stratification allows the heat removal in an optimal way and the capability to obtain comfortable conditions in warmer climate conditions (Cheong, Yua, Sekhar, Tham, & Kosonen, 2007; Chen & Olsen, 2002; Olsen, 2002).

Currently there are several ways to model the behavior of displacement ventilation: Computational Fluid Dynamics (CFD); experimentally based semi-empirical models; plume theory models; nodal models; and energy simulation software based on these two last analytical models (Graça, 2003).

CFD is being increasingly used for predicting building airflows and testing natural ventilation strategies. It has the advantage of providing air speed and temperature data at many locations throughout the flow field. With the current advances in computing power, the process of creating a CFD model and analyzing the results is becoming much less laborious, reducing the time and therefore the cost of operation. It is one of the most accurate methods to predict the DV behavior. For example, Yang (2004) found good agreement when predicting the airflow inside a naturally ventilated room, using the k-e model and Allocca (2001) compared the DV CFD simulations with experimental results acquired in a full-scale model, obtaining excellent results. However, it still requires extensive expertise and much more time than the other methods mentioned. The analysis of room geometries using weather data, spanning days or months, is usually impracticable.

Nodal model divides the room into zones and represents them by nodes (Griffith, 2002). The air movement is modeled by correlations based on experimental and CFD data. Both mass and energy conservation are imposed on the different nodes which are then solved by numerical methods. This approach allows the prediction of the temperature profile and the heat exchange between the nodes. The handicap of this model is the lack of flexibility. It is successful on simple geometries, similar to those used in the model development, but is not appropriate on other geometries since it does not model the fundamental driving mechanism

of the displacement ventilation - the plumes. Nodal models are a helpful tool for simple DV systems design due to the simplicity of the model and clarity on the assumptions made.

The plume-based models as the name suggests, rely on the plume theory, which is the fundamental mechanism of the DV (Hunt & Linden, 1999). It is possible to determine, analytically, the solution of the simplest cases, with one or two plumes. This model is accurate on the simpler models and includes the fluid mechanics behind DV, but whenever this mechanism does not prevail over the others, the applicability of this model is limited.

The implementation of nodal and plume models in Dynamic Simulation Software such as Energy Plus is a step forward in DV modeling, since it drastically increases the functionality and easiness of use of these models.

2.3 Energy Simulation Software

EnergyPlus (EP) is the most recent Energy Simulation (ES) software for buildings developed by the Energy Department of USA. It considers the tri-dimensional geometry of the building, including all the construction materials and the weather data on the building location.

All contributions to the energy balance, such as, the heat gains from occupation, equipment and lighting system, the heat gains from solar radiation, the heat exchange due to conduction and convection through walls, floors and ceilings, as well as the heat gain or loss due to infiltrations through the building facades, are considered in a dynamic way.

The energy balance for a given room (zone) is equal to

$$C_z \frac{dT_z}{dt} = \sum_{i=1}^{N_{sl}} \dot{Q}_i + \sum_{i=1}^{N_{surfaces}} h_i A_i (T_{si} - T_z) + \sum_{i=1}^{N_{zones}} \dot{m}_i C_p (T_{zi} - T_z) + \dot{m}_i C_p (T_\infty - T_z) + \dot{Q}_{sys} \quad (2)$$

where

$\sum_{i=1}^{N_{sl}} \dot{Q}_i$ is the sum of all the convective internal loads;

$\sum_{i=1}^{N_{surfaces}} h_i A_i (T_{si} - T_z)$ is the convective heat transfer from the zone surfaces;

$\sum_{i=1}^{N_{zones}} \dot{m}_i C_p (T_{zi} - T_z)$ correspond to the heat transfer resulting from inter zone air mixing;

$\dot{m}_i C_p (T_\infty - T_z)$ is the heat gain or loss due to infiltration of outside air;

$C_z \frac{dT_z}{dt}$ is the energy stored in the zone air;

and \dot{Q}_{sys} is the energy removed by the system

$$\dot{Q}_{sys} = \dot{m}_{sys} C_P (T_{Sup} - T_z) \quad (3)$$

Equation 3 assumes that the zone supply air mass flow rate is exactly equal to the sum of the airflow rates leaving the room. Typically the capacitance C_z , would be only associated with the air, but thermal masses that are assumed to be in equilibrium with the zone air could also be included in this term.

Equation 2 is solved by numerical integration using a time step smaller than the simulation time step, typically around 0.1 - 0.25 hours. The smaller this step is, the smaller will be the integration error, but the longer will be the computation time.

Although the zone energy balance is the key equation of EP, it is able to do much more. EP simulates in detail the performance of integrated building energy systems (constant and variable air volume systems, radiant systems, etc.) and main pieces of equipment (coils, fans, pumps, etc.) can also be simulated (DOE EnergyPlus, 2005; DOE EnergyPlus, 2007). EP has also several models to predict the thermal comfort of the building occupants.

The level of detail in the simulation output allows a deep assessment of all the data related with an HVAC system and It is possible to control the system operation, diagnose possible problems and test different configurations. ES predicts the energy consumption of the building through hourly dynamic computation of the energy balance. The output includes not only the global building consumption data but also detailed outputs related to each thermal zone.

With such a level of detail in the results it is possible to study modifications in order to improve the building performance, considering both the investment and the resulting benefits. The use of this software might be a powerful tool to evaluate energy efficient solutions in the building design process before installing them on the real building (Olsen, 2002).

2.3.1 Displacement ventilation models

Initially Energy Plus was developed to consider only mixed ventilation systems but it was soon modified to be able to use other models (Graça, 2003; Mundt E. , 1996). At the moment there are two DV models: the Mundt model and the UCSD Displacement Ventilation Room Air Model. A third DV model, UFAD UCSD Interior Model, was developed but it is limited to the particular case where air is supplied through an air plenum under the floor.

2.3.1.1 Mundt Model

Mundt model is a nodal based model developed by Mundt in 1996. It considers that a linear temperature gradient between the floor and the ceiling is an accurate way to preview the temperature stratification in a room. An air energy balance on the node near the floor provides the temperature of the air on that subzone, $T_{AirFloor}$, while the upper temperature, $T_{Leaving}$, is obtained from another node that comes from the usual overall air system energy balance (DOE EnergyPlus, 2005). The energy balance near the floor was modified to include convection heat gains from equipment and from ventilation and infiltration

$$\rho C_p \dot{V} (T_{AirFloor} - T_{Supply}) = h_{c,Floor} A_{Floor} (T_{Floor} - T_{AirFlow}) + Q_{ConvSourcesFloor} + Q_{InfiltrationFloor} \quad (4)$$

where ρ is the air density, C_p is the air specific heat at constant pressure, \dot{V} is the air flow rate, T_{Supply} is the air supply dry bulb temperature, $h_{c,Floor}$ is the convection heat transfer coefficient, A_{Floor} is the surface area of the floor, T_{Floor} is the surface temperature of the floor, $Q_{ConvSourcesFloor}$ is the convection from internal sources near the floor and $Q_{InfiltrationFloor}$ is the heat gain from infiltration or ventilation. The previous equation can be rearranged to compute $T_{AirFloor}$

$$T_{AirFloor} = \frac{\rho C_p \dot{V} T_{Supply} + \sum h_{c,Floor} A_{Floor} T_{Floor} + \dot{Q}_{ConvSourceFloor} + \dot{Q}_{Infiltration,Floor}}{\rho C_p \dot{V} + \sum h_{c,Floor} A_{Floor}} \quad (5)$$

The upper temperature is computed by

$$T_{Leaving} = \frac{-Q_{Sys}}{\rho C_p \dot{V}} + T_{Supply} \quad (6)$$

and finally the temperature gradient is given by

$$\frac{dT}{dz} = \frac{T_{Leaving} - T_{AirFloor}}{H_{return}} \quad (7)$$

where H_{return} is the height of the room.

2.3.1.2 UCSD Displacement Ventilation Room Air Model

The UCSD Displacement Ventilation Air Room model (UCSD-DVAR) was developed in University of California San Diego by Graça (2003). This three-node model considers the fundamental DV mechanism, allowing an improved prediction of the overall system performance.

UCSD-DVAR is one of the Energy Plus non-uniform temperature zone models to provide the evaluation of air-conditioning techniques that take advantage of the stratified room air temperatures (DOE EnergyPlus, 2005). This model will be described in detail in Chapter 3.

2.3.1.3 UCSD Under Floor Air Distribution Model

The UCSD Under Floor Air Distribution Model (UCSD-UFAD) air distribution model in EP is very similar to the UCSD-DVAR model. It is based on plume theory and considers that there is vertical temperature stratification. In UFAD systems, air is supplied through an under floor plenum at low pressure through specific diffusers. As in the case of DV, UFAD systems have a great potential in energy savings due to higher supply air temperature, low static pressure, and cooler conditions in the occupied subzone than in the upper subzone.

It is very complex to model these systems, since the supply and return plenums must be modeled with high accuracy, and additional units need to be defined (return air Bypass and terminal units). The most obvious differences between UCSD DV and UCSD UFAD are the air diffusers location and the inexistence of a floor subzone. This model also has a slight different approach, instead of considering a vertical gradient between the existing subzones it assumes a constant temperature on the upper zone and on the lower occupied zone.

2.3.2 Variable Air Volume Fan System

EP can model Constant Volume (CV) and Variable Air Volume (VAV) fan systems. CV systems use a constant inflow volume and adjust the temperature to condition the controlled zone. A VAV system does exactly the opposite; it fixes the inflow temperature and changes the flow rate in order to maintain the desired temperature and humidity inside the room. A VAV can be schematized as in Figure 6.

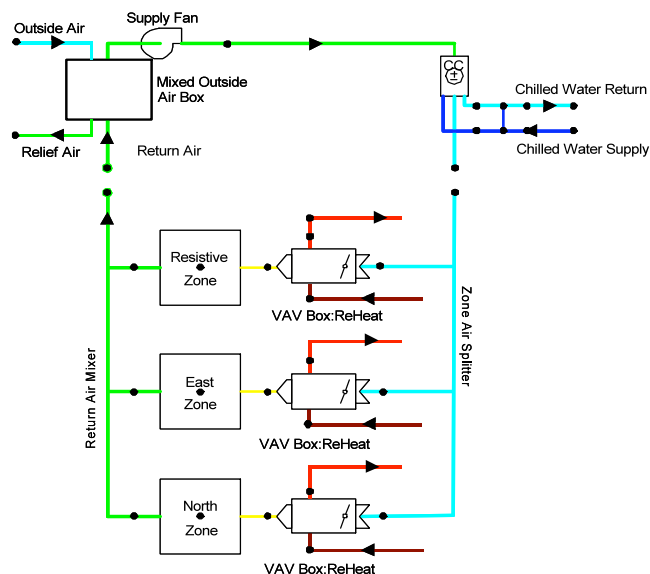


Figure 6 - Variable Air Volume system diagram

The Air Loop, represented in green on Figure 6, includes the Mixed Air System, the Supply Fan, the Cooling Coil and the Heating Coil. In the Mixed Air System, part of the air returned from the room is relieved to the outside while an equal volume of outside air mixes with the rest of the returned air. The resultant air passes through the Supply Fan and goes towards the Cooling Coil and Heating Coil, where it will exchange heat. Leaving the Heating Coil, the air enters the Zone Equipment Loop, shown Cyan on Figure 6. This loop contains the splitter that will split the air to the various zones. Each zone has a damper, to control the inflow air volume and, if the system is equipped with a reheat controller, it will also contain a reheat Coil. The air from the splitter enters the zone, where it will be then exhausted and returned to the mixed air box.

2.3.3 Thermal Comfort

Comfort can be defined as the state of spirit that expresses the satisfaction with the surrounding conditions. It has many components and one of the most important is Thermal Comfort (TC). TC is the study of the human body reaction, to thermal stimulations. Many variables influence TC, including: body temperature; ambient temperature; body external surface (skin); mean radiant temperature; relative humidity; air velocity; clothing factor; and the subject's metabolic activity. Since the normal body temperature is around 37°C, which is usually above the ambient temperature, human body is constantly losing energy to the surrounding environment. In order to balance this loss the body has internal mechanisms to produce energy, its metabolism. Thermal comfort is achieved whenever the following condition is verified.

$$\text{Energy produced by the body} = \text{Energy losses to the environment}$$

There is no combination of the above-mentioned variables that could grant that everyone in a given population is comfortable and in fact even for ideal conditions there is generally 5% of dissatisfied subjects.

EP has various models to preview TC inside a certain zone, but Fanger's model is the most well known. It was developed by Fanger in Kansas State University and it considers an enormous list of variables (DOE EnergyPlus, 2005). The index of thermal comfort also known as Predicted Mean Vote (PMV) is obtained following the ISO 7730 standard. It results from numerous experiments involving human subjects in various environments. The PMV is a scale between the values of -3 to 3, representing the extreme values for discomfort by cold and by heat, respectively. The comfort region on this scale lay between -0.5 and 0.5. Figure 7 shows the comfort region on the PMV scale.

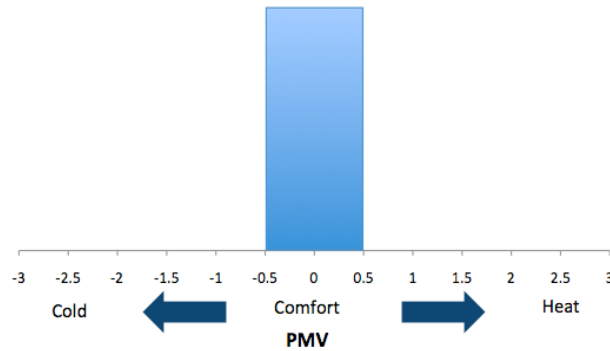


Figure 7 - Predicted mean vote (PMV) comfort scale

The model is based upon an energy analysis that takes into account all the modes of energy loss from the body, including: convection and radiant heat loss from the external surface of the clothing; heat loss by water vapor diffusion through the skin; heat loss by evaporation of sweat from the skin surface; latent and dry respiration heat loss; and heat transfer from the skin to the outer surface of the clothing. The model assumes that the person is thermally at steady state with his or hers environment (DOE EnergyPlus, 2005).

2.4 Computational Fluid Dynamics

Computational Fluid Dynamics (CFD) is undoubtedly the most powerful tool in predicting the airflow (Zhai, 2003). It solves numerically the governing conservative equations of the fluid flow, and can predict detailed time-dependent and three-dimensional distributions of the air velocity, pressure, temperature, relative humidity and contaminant concentrations. These results can be used to determine the IAQ, or to evaluate ventilation systems performance, by predicting the spatial temperature distribution inside a room, or the air velocities near an occupant (Deevy, Sinai, Everitt, Voigt, & Gobeau, 2007).

With the growing computational power, the use of CFD in buildings design is becoming very common. Some studies of natural ventilated buildings have been done (Ji, Cook, & Hanby, 2005, Sousa, Madureira, Gomes, & Lopes, 2006).

The indoor airflow is, in most cases, turbulent. CFD can predict turbulent flows, using Reynolds Average Navier-Stokes (RANS) modeling. There are many models within this type of turbulence models but the most used is the $k-\varepsilon$ turbulence model, which couples two equations, one for turbulent energy density (k) and other for the turbulent dissipation rate (ε).

The highly accurate and detailed results provided by the CFD, make it a very interesting tool to study the flow and performance of naturally driven ventilations systems as, for instance, DV systems, which has been studied by many authors. Howel and Pots (2002)

studied the importance of the radiation and relative humidity on DV systems; Müller and Kriegel (year unknown) presented a study with changes to the existing $k-\epsilon$ model to enhance the DV prediction. Also using CFD, Law and Chen (2007) studied the performance and applicability of a DV system in a room used for workshops. Song et al. (2008) used CFD to develop a new zonal modeling approach for predicting the ventilation system performance. CFD also allowed investigating the influence of the air supply location (Lin Z. , Chow, Tsang, Fong, & Chan, 2004).

CFD is the most powerful tool, of those above mentioned, to preview the behavior of a DV system, but it requires much more computational power and time than the energy simulation software. Furthermore, it is not feasible to study the behavior of a building in a dynamic way, with weather data for entire days, weeks or months as it is with EP.

3 Technical Description and Results

3.1 Model Description

In order to accomplish the objectives proposed, it was necessary to use one of the EP DV models. The model used was the UCSD DVAR, because it seemed to be the most appropriated. As it was above described this is a model based on plume theory. The problem is solved considering an n-equal plume approximation; this means it considers all plumes to have the same strength. Obviously, in a real room, the generated plumes are not equal, and even if they were, there would always be the risk of coalescence. But generally if they are half a meter apart from each other this can be a fair approximation (Graça, 2003; DOE EnergyPlus, 2005). For the case of n-equal and non-coalescent plumes, the vertical airflow at a certain height, is given by

$$\dot{V} = nCB^{1/3}z^{5/3} \quad (8)$$

where \dot{V} is the plume volume flux in m^3/s , n is the number of plumes, z is the height in m , B is the buoyancy flux in m^4/s^3 . C is a constant given by

$$C = \frac{6}{5}\alpha\left(\frac{9}{10}\alpha\right)^{1/3}\pi^{2/3} \quad (9)$$

where α is the plume entrainment constant ($\alpha = 0.13$, (Graça,2003)). Considering an ideal gas, the buoyancy flux will result in

$$B = \frac{g\dot{Q}}{\rho C_p T} \quad (10)$$

where g is the acceleration of gravity in m/s^2 , T is the air temperature in $^{\circ}C$, ρ is the density of air in kg/m^3 , \dot{Q} is the heat input rate in W and C_p is the specific heat capacity of air in $J/kg^{\circ}C$.

The plume volume flow rate increases in a 5/3 exponential with the height z , therefore there will always be an height, h , for which \dot{V} matches the inflow rate, F . Replacing F and h in equation (8) and solving

$$h = \frac{F^{3/5}}{C^{3/5}B^{1/5}} \quad (11)$$

To predict the transition height the software estimates the temperatures on the mixed zone, the occupied zone and the temperature near floor. To perform these calculations the

software will first need to calculate the total of convective gains, on each zone, using equations 12 and 13. The total convective gains inside the room are computed using

$$\dot{Q}_{OccZone} = \dot{Q}_{OccConvective} + \dot{Q}_{equipConvective} \quad (12)$$

$$\dot{Q}_{MxZone} = \dot{Q}_{LightsConvective} + \dot{Q}_{RadConvective} \quad (13)$$

$$\dot{Q}_{TotalConvective} = \dot{Q}_{OccZone} + \dot{Q}_{MxZone} \quad (14)$$

where subscript *Occ* stands for occupants, *equip* for equipment, *lights* for lighting system, *Rad* for radiation *OccZone* for occupied zone and *MxZone* for mixed zone.

The effective convection heat removed per plume results in

$$\dot{Q}_{Plumes} = (1 - G_{FR}) \dot{Q}_{Total} \quad (15)$$

$$\dot{Q}_{PerPlume} = \frac{\dot{Q}_{Plumes}}{N_{Plumes}} \quad (16)$$

where G_{FR} is the convective heat gain fraction that remains within the occupied zone, N_{Plumes} is the number of plumes defined by the user and \dot{Q}_{Plumes} is the heat removed by the plumes from the occupied zone. A first estimation of the transition height is given by

$$h = 24.55 \left(\frac{MC_{PTotal}}{\rho_{air} C_{PAir}} \frac{1}{N_{Plumes} \dot{Q}_{PerPlume}^{1/3}} \right)^{3/5} \quad (17)$$

After this first estimation, the software performs an iterative process consisting in the following three steps:

- In a first step the software predicts the convection heat transfer coefficient and the temperature for each surface inside the room, accounting for their position, which means, considering the adjacent zone and the incident radiation on those surfaces.
- The transition height is then recalculated in the second step.
- The third step consists in the calculation of the three zone temperatures.

All the computations described above assumed that conditions were favorable to DV, which is not necessarily true. To check the validity of the assumption, EP needs to verify if the three following conditions are verified.

$$T_{mixed} > T_{Occupied} \quad (18)$$

$$MC_{P_{Total}} \geq 0 \quad (19)$$

$$h_{Transition} \geq h_{FloorZone} + z_{Min,OccZone} \quad (20)$$

If the conditions are not verified, the software considers that the system is mixed and thus replaces the DV calculations by MV calculations.

3.2 Simple Model Building

In order to study the applicability of the EP model, a simple model building was used. It was developed using the graphical user interface *Design Builder 1.4*. It is a single story office building, with 400 m^2 area and 4 m height. Figure 8 shows an illustrative image of the model building in question. It was chosen an office building, since this kind of buildings has the suitable conditions to operate in DV (Hensen, Hamelinck & Loomans).



Figure 8 - Illustrative image of the model building

3.2.1 Model Building Description

3.2.1.1 Geometric Model

The model building has a window (with 32 m^2) facing south and equipped with a shadowing device (overhang with 20 cm) to reduce the incident direct radiation during the summer season. The constructive solutions are also very important in the efficiency of the building. Tables 1 to 3 list the thermal properties of the materials used in the various constructive solutions where k is conductivity of the material, C_p is heat capacity at constant pressure and U is the heat transfer coefficient.

Table 1 - Table with the thermal properties of the floor materials

Material	C_p J/kg/K	Thickness m	k W/m/K	R $\text{m}^2\text{C/W}$	U W/m ² /K
Wooden Flooring	1200	0.03	0.14	0.21	
Screed	840	0.07	0.41	0.17	
Cast Concrete	1000	0.10	1.13	0.09	0.35
UF Foam	1400	0.08	0.04	2.00	

Table 2 - Table with the thermal properties of the ceiling materials

Material	Cp J/kgK	Thickness m	k W/mK	R m ² °C/W	U W/m ² K
Plywood	1420	0.01	0.150	0.07	
Glass Wool	840	0.13	0.040	3.25	
Cast Concrete	1000	0.10	0.380	0.26	0.25
Air Gap	1000	0.20	0.003	0.16	
Plasterboard	896	0.01	0.250	0.04	

Table 3 - Table with the thermal properties of the wall materials

Material	Cp J/kgK	Thickness m	k W/mK	R m ² °C/W	U W/m ² K
Brickwork	800	0.10	0.840	0.12	
Extruded Polystyrene	1400	0.08	0.034	2.35	0.35
Concrete Block	1000	0.10	0.510	0.20	
Gypsum Plasterboard	1000	0.01	0.400	0.03	

3.2.1.2 Climate model

The city Porto, Portugal was chosen for the model building simulation. For ES the hourly weather information considered was the reference data of the city of Porto from the EP database, including the external temperature, the relative humidity, the solar radiation (both direct and diffuse) and the wind direction and speed. Figures 9 to 12 show the charts of the typical monthly values for the above-mentioned variables.

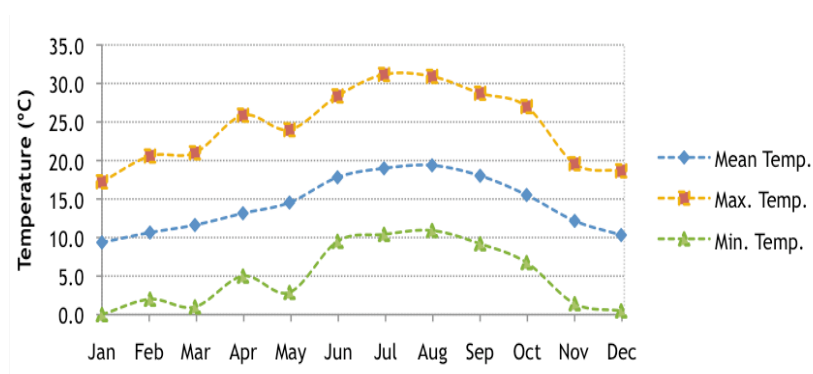


Figure 9 - Monthly maximum, minimum and mean temperatures.

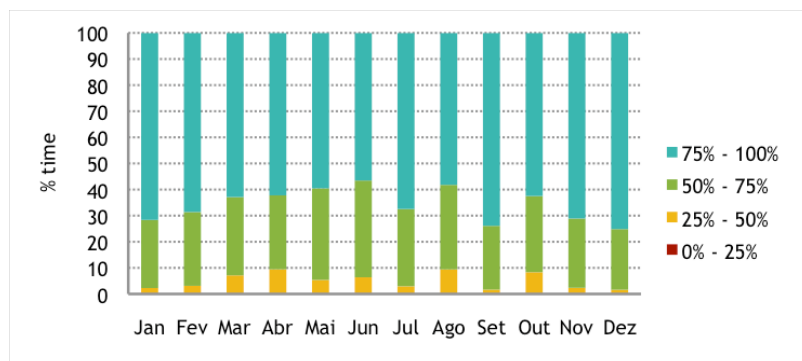


Figure 10 - Monthly time distribution of a given relative humidity.

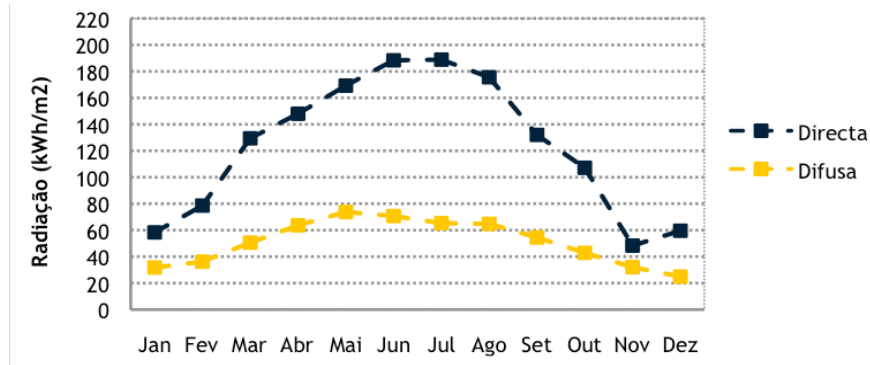


Figure 11 - Total monthly evolution solar radiation, both diffuse and direct

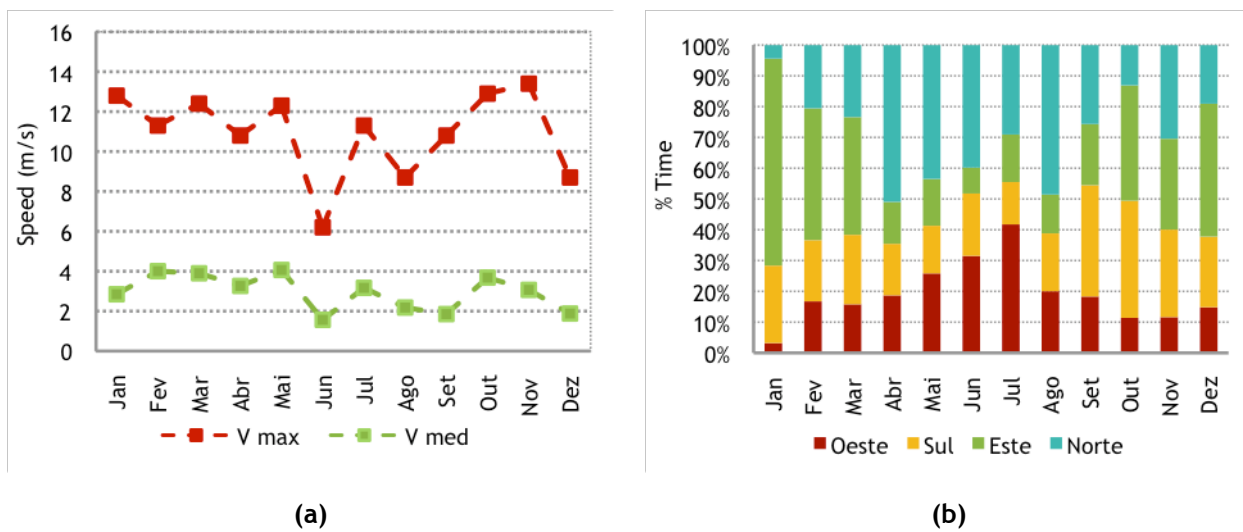


Figure 12 - Monthly evolution of wind speed (a) and direction (b).

3.2.1.3 Activity model

Another important factor, for the dynamic simulation, is the building activity model, which is related to usage and purpose. The activity model includes the occupation profile, as well as the equipment and lighting system. For this work it was chosen the reference data defined in the current Portuguese building code - RSECE (Regulamento dos Sistemas Energéticos de Climatização de Edifícios), for this kind of buildings.

The model was considered as an office space, using the RSECE predicted densities and profiles. Table 4 lists the respective densities of occupation, equipment and lighting system. Office working hours are assumed between 09:00 and 19:00. Office buildings are particularly interesting for the DV. They normally have large heat gains resulting from the occupants and from their computers. Typically the occupant and their computer are very close to each other and therefore only one plume for both is considered.

Table 4 - Densities of occupation, equipment and lighting equipment predicted by RSECE

	Density
Occupation	15 m ² /person
Equipment	15 W/m ²
Lighting equipment	10 W/m ²

The subjects inside the building are considered to be sitting/writing, for which activity the predicted heat gain is 117 W/m² (ASHRAE, 2005).

Detailed information about the profiles predicted by RSECE for the activity model of the building, such as Schedules of occupation, lighting system and equipment use are listed in the Appendix 1.

3.2.1.4 Heating, Ventilation and Air Conditioning (HVAC) Model

The conditioning model assumes the implementation of primary and secondary conditioning systems to simulate all the equipment and to compute the energy consumptions.

The primary system refers to the equipment where chilled and hot water are produced to supply the energy needs of the system. For this building it was considered that the chilled water was produced in a chiller and the hot water was produced in a boiler.

The secondary conditioning system is responsible for the inside temperature control and for the supply of outside air, to dilute pollutants in order to ensure the indoor air quality. All equipments and processes associated with the Air Handling Unit were also considered.

To simulate the secondary system it was considered the following:

- Supply and return air in each zone;
- The supply air temperature of the air from the air handling unit is 21°C for cooling and heating. Note that this is a DV system and therefore it is not desirable to use the ventilation air to heat the room.

To simulate the ventilation units, the *FAN: SIMPLE: VARIABLE VOLUME* model was used. The cooling and heat coils simulation was done with the EnergyPlus models: *COIL: WATER: COOLING* and the *COIL: WATER: SIMPLE HEATING*, respectively.

The simulation of this secondary system, allows quantifying the heating and cooling processes on the coils, the humidification and dehumidification, as well as, the ventilation and pump electric consumption. It also accounts for the inefficiency of the equipments and, as a consequence, for the energy loss to the fluid.

Once it is not recommended to heat the room with ventilation air, in DV (see Section 2.2), it was necessary to add an external heating unit. A radiant floor was chosen and simulated using the *LOW TEMP RADIANT SYSTEM: HYDRONIC* model.

3.2.2 Parametric Study

The UCSD-DV model has many user-defined parameters. Additional inputs for this model are: number of plumes; thermostat height; gain distribution schedule; comfort height; and the minimum temperature difference between the mixed zone and the occupied zone. In order to choose the appropriate values, some parametric studies were carried out.

The minimum temperature difference, the number of plumes and comfort height were not studied in this section. Note that the comfort height and the minimum temperature difference do not affect the system, the first represents the height at which the temperature comfort is measured while the second works as a flag, meaning that DV computations will only be done if the temperature difference between the mixed subzone and the occupied zone is larger than this value. The number of plumes was considered to be always one since it is a good approximation for offices.

3.2.2.1 Thermostat height

The thermostat height (TH) defines the position of the temperature control system, and it should be below the transition height. The system senses the room temperature through the thermostat and modulates the supply airflow rate to control the occupied zone temperature. To study the effect of this variable, different values of TH were used, and the respective transition height calculated along a given day. In Figure 13 the change in transition height with the thermostat height is shown for both a winter and a summer day.

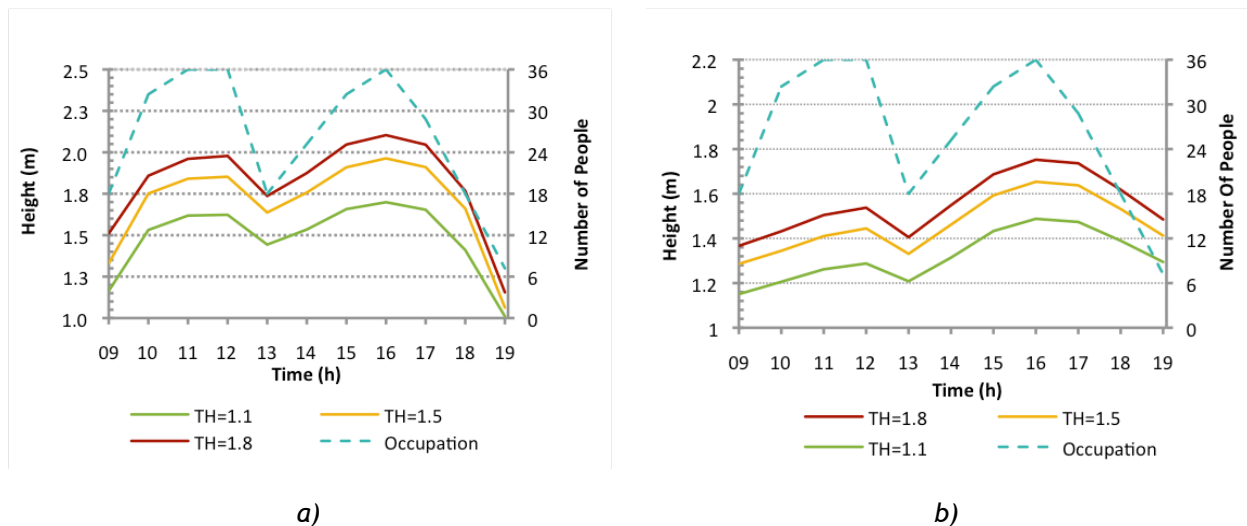


Figure 13 - Transition height, for three thermostat heights, during a winter day (a) and a summer day (b).

The transition height increases with the TH. In fact increasing the thermostat height will force the transition height to rise, because the thermostat must be within the occupied zone, and due to stratification, the higher the thermostat is, the higher will be the supply air flow rate, resulting in a higher transition height. The transition height follows the occupation

profile. This happens because the heat that has to be removed increases with the occupancy, because the occupation, equipment and lights profiles are very similar.

Comfort was also monitored for the occupied zone, shown in Figure 14 for the three different thermostat heights.

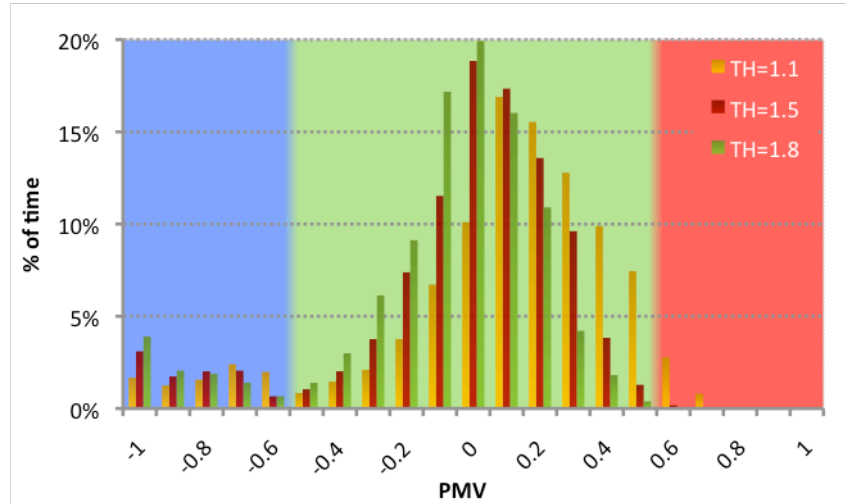


Figure 14 -Percentage time of comfort for the three thermostat heights

The percentage of time comfort histogram is centered at zero for the transition height of 1.5 m. For a lower TH, the histogram moves to the warmer side, meaning that there will be more time of discomfort by heat. On the other hand, if the thermostat height is increased the histogram moves to the colder side, meaning that there will be more time of discomfort by cold. This is an expected result, given that the room temperature is stratified, and positioning the controller higher (lower), leads to a larger (smaller) volume below that height with a lower temperature.

Another important parameter studied was energy consumption. Figure 15 shows the annual cooling consumption for the three different positions of the thermostat.

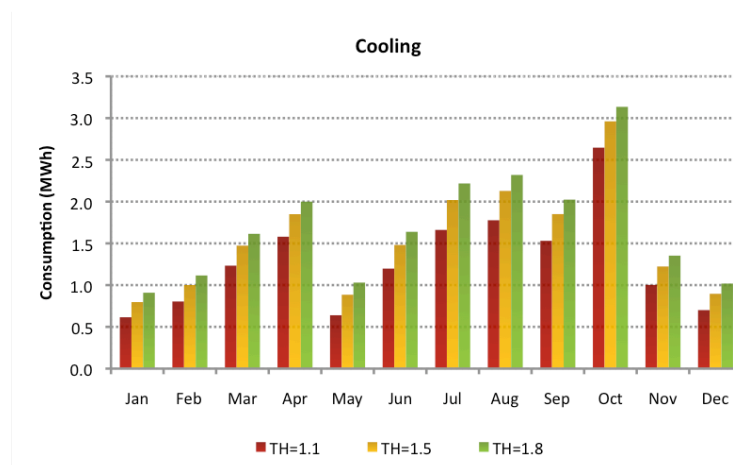


Figure 15 - Energy consumption for cooling for the three studied thermostat positions

As shown in Figure 13 the transition height increases with the TH, and thus the conditioned volume (occupied zone) is also larger. As a consequence, the consumed energy for cooling is larger. The room is heated by an external system, a radiant floor, and therefore the corresponding energy consumptions are not relevant here.

The thermostat was placed at 1.5 m, since it was the height that had the best results for the desired proposes.

3.2.2.2 Gain Distribution

The influence that the fraction of convective heat, that remains on the occupied zone, has on the simulation results was studied, mostly because it is an empirically parameter. Nielsen studied this parameter and concluded that, for office equipment, it should be between 0.3 and 0.5 (Arens, 2000). Increasing the Gain Distribution (GD) factor, the energy that would remain in the occupied zone would also increase. As a consequence, the inflow air needed to conditioning the zone would be bigger. Knowing that the volume flow rate, dragged by the plumes, will increase with the height, there will always be a height that this flow rate will match the zone inflow - transition height. As a result of these conditions it was expected that the cooling energy consumptions and the transition height would be affected. The results obtained are presented in Figure 16 to 18.

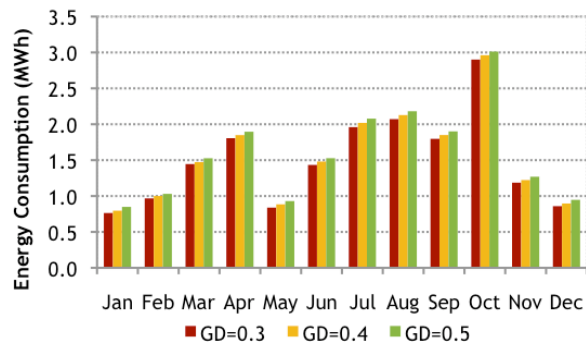


Figure 16 - Energy consumption for cooling for the three studied GD fractions

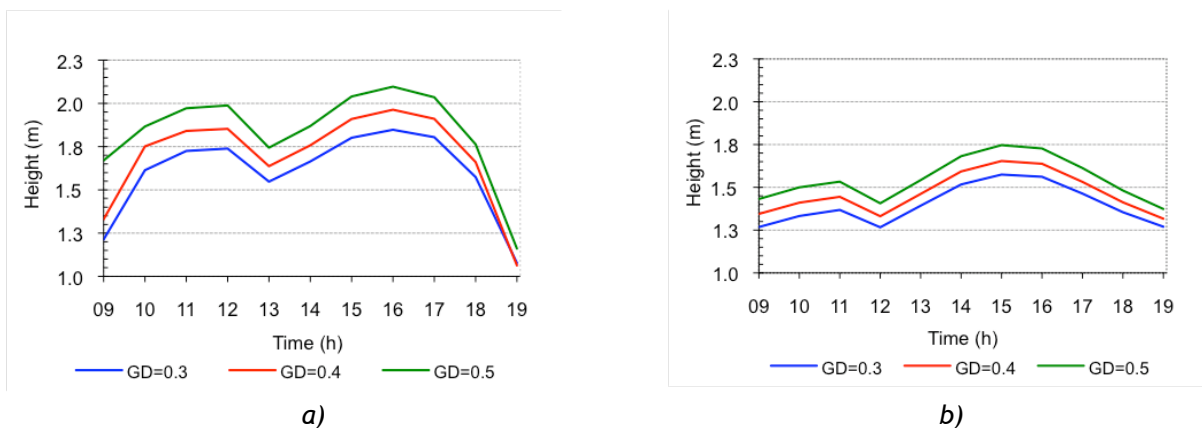


Figure 17 -Charts with the transition height, for the three different GD, during a winter day (a) and

during a summer day (b)

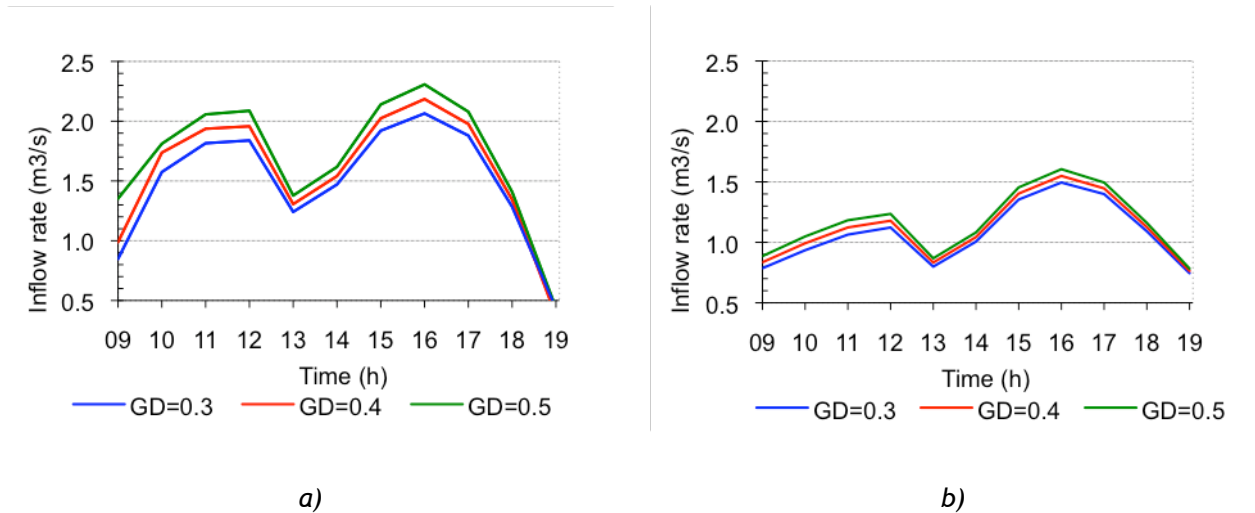


Figure 18 -Charts with the Inflow rate, for the three different GD, during a winter day (a) and during a summer day (b)

It is possible to observe that all the three monitored parameters increased with the GD fraction, with a stronger difference on the transition height. The Inflow air increased during the winter, but during the summer it barely changed, probably because the amount of inflow air required during the summer is relatively smaller, and consequently masking the differences. The increased supply airflow rate in the winter results from the smaller gradient between the supply air temperature and the room set point in this season.

3.2.2.3 Internal Gains

The effect of the internal gains in the simulation results was also considered. To do so, the internal gains were changed while all the other conditions were maintained. As happened with the GD, the internal gains have direct impact on the transition height, inflow rate, and energy consumption, because it also has more energy to remove, needing an increased inflow rate. The internal gains considered for this study were 10W/m², 15W/m² and 20W/m², and the results of the simulations are presented in figures 19 to 21.

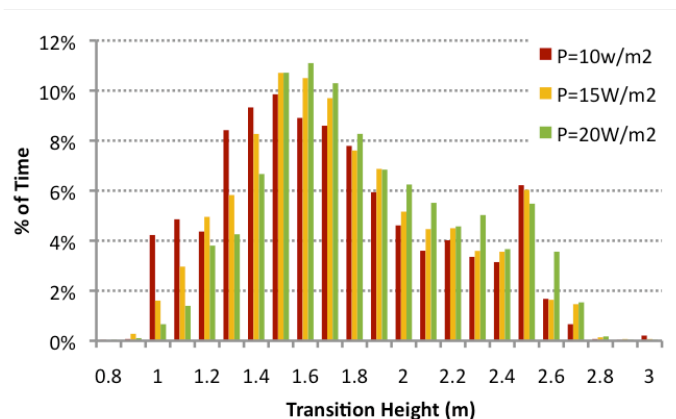


Figure 19 - Time distribution of the transition height for the three studied heat gains

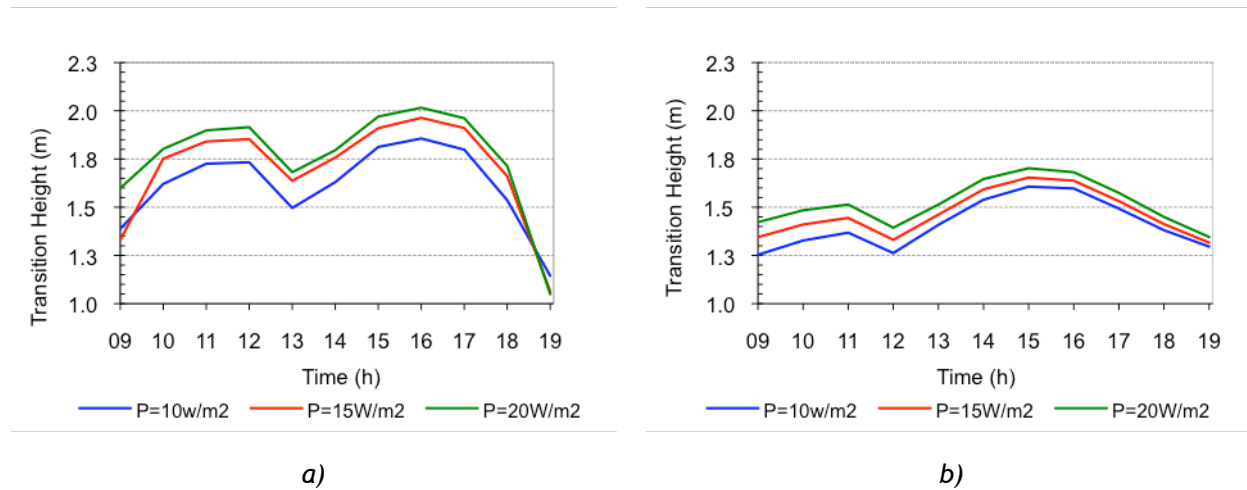


Figure 20 - Charts with the transition height, for the three different heat gains, during a winter day (a) and a summer day (b)

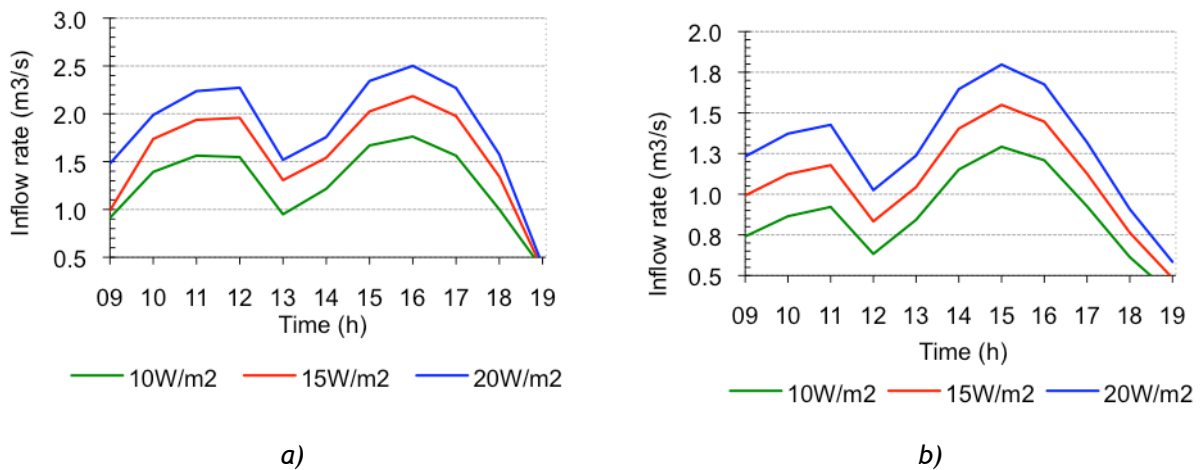


Figure 21 - Charts with the inflow rate, for the three different heat gains, during a winter day (a) and a summer day (b)

The histogram on Figure 19 shows the performance of the system for the three cases considered, evaluating the transition height distribution along the year. It is important to remark that the transition height decreases with the decrement of the heat gains inside the room, this is understandable, since the increase of the heat gains will enlarge the cooling needs, and therefore the supply airflow. As a consequence the cooling energy consumption will be augmented.

Since this is a VAV system that maintains the temperature and varies the volume flow rate to match the energy need, the supply airflow rate increase (see Figure 21) is justifiable by the same reason as the energy consumption.

3.2.3 EnergyPlus Simulation Results

The above parametric study helped to choose the simulation parameters (Table 5) for the DV model, in order to obtain the desired operative conditions.

Table 5 - Parameters used on the UCSD-DV model

Number of Plumes per occupant	1
Gain distribution fraction	0.4
Thermostat height	1.5
Comfort height	1.6
Minimum temperature difference between the mixed and occupied zone	0.4

The simulation results obtained for the DV model were compared, when possible, with the results of an equivalent mixing ventilation system. The conditions for both DV and MV were kept as similar as possible, and are shown in Table 6.

Table 6 - Simulation conditions for displacement and mixing ventilation

	Mixing Ventilation	Displacement Ventilation
Inflow Temperature	20.5 °C	20.5 °C
Winter Set-Point (SP)	22.0 °C	22.0 °C
Summer Set-Point (SP)	25.0 °C	25.0 °C
Radiant floor Heating SP	22.0 °C	22.0 °C
Radiant floor Cooling SP	Off	Off
HVAC System Availability	08h-19h	08h-19h

The operative temperatures of both systems were calculated hourly for an entire year, but to simplify the presentation and discussion of the results, typical winter and summer days were chosen. The charts presented in Figures 22 and 23, show the zone temperature for MV, and the temperatures of the each sub-zone for DV, during the representative period.

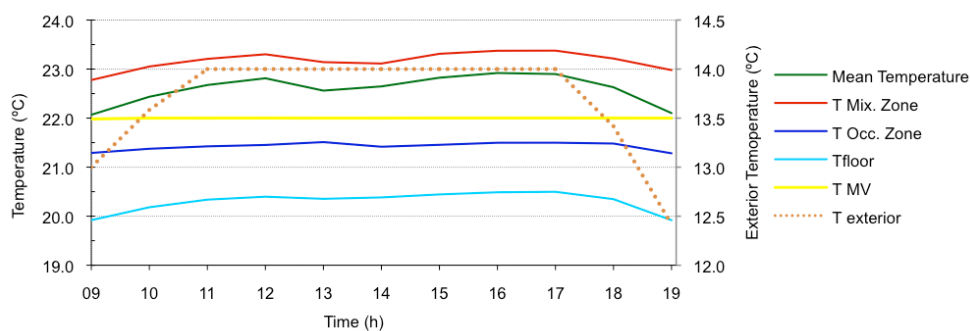


Figure 22 - Zone temperatures during a representative winter day for MV and DV systems.

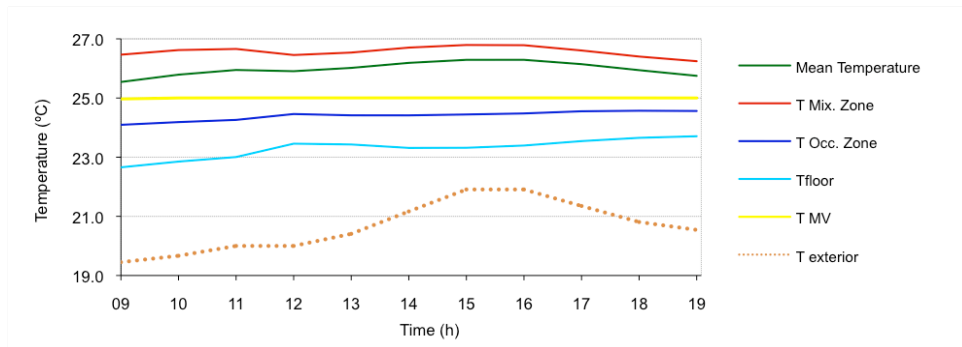


Figure 23 -Zone temperatures during a representative summer day for MV and DV systems.

It is possible to observe that the temperature of the occupied zone is slightly below the defined set point on both cases. This happens, mainly because the system controls the room temperature at the thermostat height and due to the stratification, the occupied zone underneath that position will be colder than the set point, resulting in a reduction of the mean temperature of that subzone. It is important to note that the temperature measured at the thermostat height matches the set point temperature (25 °C for summer and 22 °C for winter). Figures 22 and 23 also show an oscillation on the occupied zone temperature, more perceptible during the summer (see Figure 23). This fluctuation occurs, mainly because the conditioning volume (Occ. zone) is not constant. It depends on the transition height that varies with the inlet conditions that are not constant in time, as it is possible to see in Figure 24. Note that the oscillation verified during the summer is very similar to the variation of the conditioning volume (see Figure 24b).

Given that the fan system modeled was the VAV, described in Section 2.3.2, the inlet volume flow rate for both systems was monitored and compared, in the same typical period for winter and summer. The results are illustrated in Figure 25

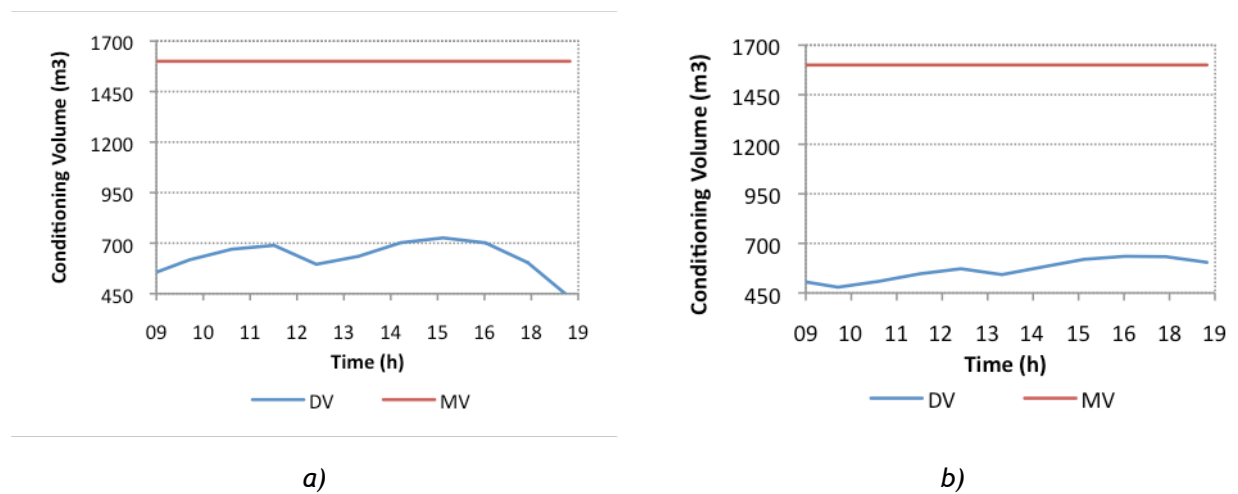


Figure 24 - Variation of the conditioning volume during a typical winter day a) and a summer day b)

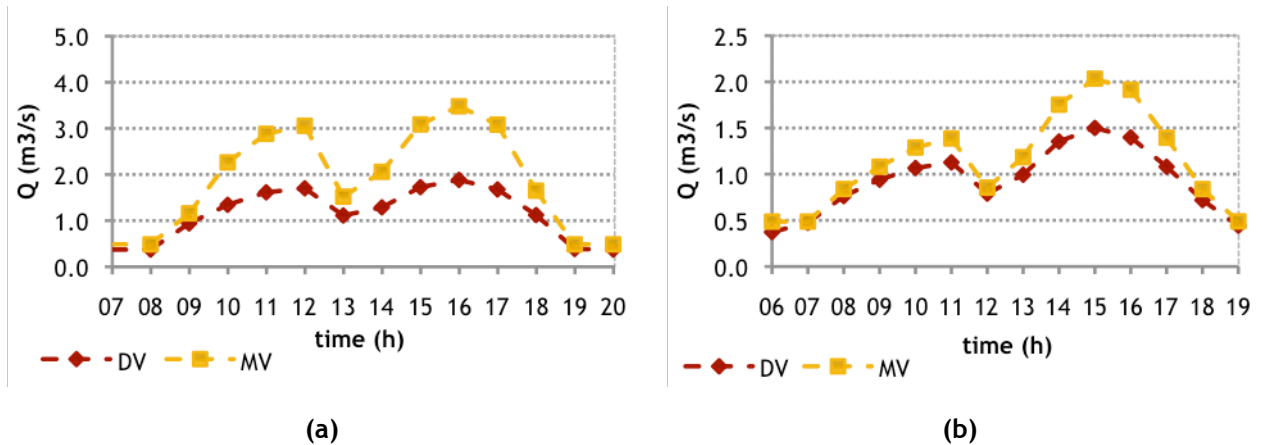


Figure 25 - Inlet volume flow rate during a typical winter day a) and summer day (b).

The inlet volume flow rate is similar for both systems, but it is generally slightly larger on the MV system. The smaller inlet airflow in DV is associated with the reduction of the conditioning volume to the occupied subzone (below the transition height). Note that there is a point where the MV inflow is almost the same as in the DV. This happens, because there is a sudden decrease on the internal gains.

The difference on the inlet flow should also be verified in the energy consumption, because it increases with the amount of conditioned air. This is evident in the histograms of Figure 26 and 27 that illustrate the amount of energy spent for heating and cooling.

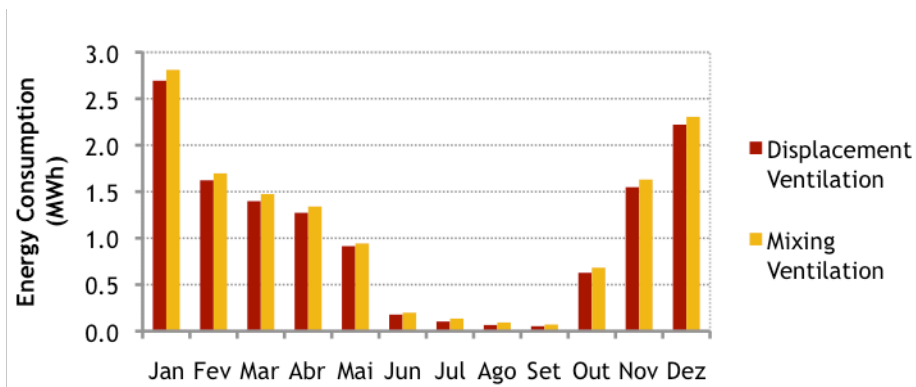


Figure 26 - Monthly heating energy consumption for DV and MV systems

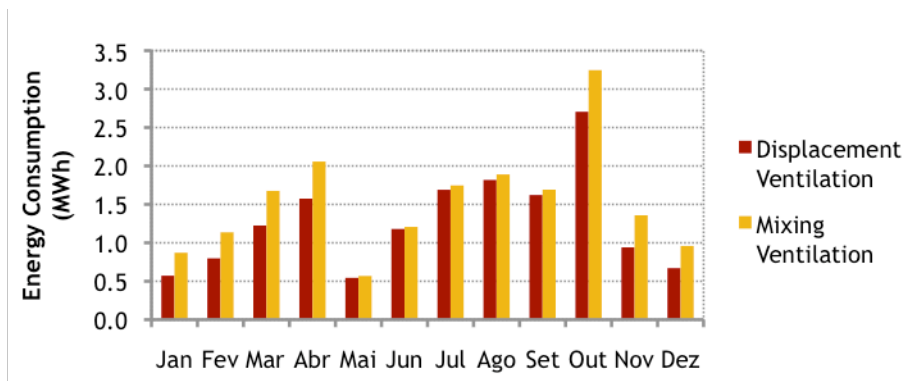


Figure 27 - Monthly cooling energy consumption for DV and MV systems

MV requires more energy for cooling and for heating. The difference is less noticeable in the heating energy because it is masked by the energy used for the radiant floor, which is much bigger than the energy used in the ventilation system. Figure 28 illustrates the energy spent for heating, cooling and ventilation for the MV and DV systems.

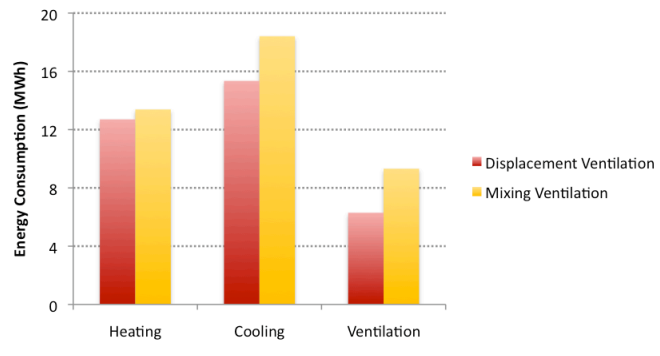


Figure 28 - Annual energy consumptions for heating, cooling and ventilation

Using DV the ventilation energy reduces 32%, the cooling energy reduces 20% while the heating energy will only reduce 5%. On both cases, heating is mainly provided by a radiant floor, resulting in similar energy consumption for both systems.

The comfort levels on both systems were monitored and are shown in Figure 29.

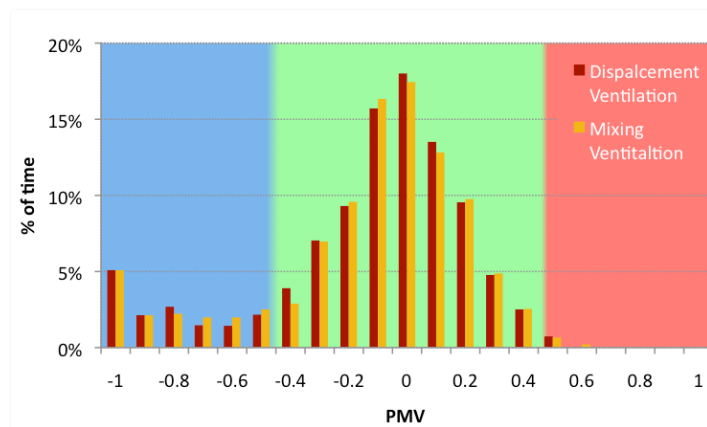


Figure 29 - Histogram with comfort time percentage for both systems

Although there are some slight differences in the histogram, the percentage of comfortable time is very similar on both systems. The MV system has 89% of the time within the comfort zone, while the DV system reaches 90% of comfortable time for the same conditions. Knowing that the acceptable simulation error range is about 10%, this difference is meaningless.

It is important to state that for the almost the same comfort, DV uses much less energy than the equivalent MV system.

3.3 Validation of EnergyPlus Model with CFD

3.3.1 ES Model Description

The main objective of this chapter is to compare the EP predictions with the results obtained in the CFD simulation. The model used in these simulations, had to be simplified and consequently the window facing south was removed.

As mentioned in Section 2.4 using CFD, it is impracticable to simulate a building dynamically during weeks or months, so the weather data file was also changed, to obtain constant conditions, allowing the EP simulation to reach a *Pseudo Steady State*. The constant conditions defined on the tuned weather file are listed in Table 7.

Table 7 -EP tuned weather file conditions

External Temperature	29 °C
Wind Speed	No Wind
Radiation	No external solar radiation
Dew Point	17.6 °C
Pressure	1 atm

The steady state obtained with this simplified EP simulation, was the starting point for the CFD model, since it allowed obtaining all the boundary conditions needed for the CFD simulation, including the supply air flow rate and temperature: supply airflow rate equal to 1.66 m³/s and supply air temperature equal to 20.5°C

3.3.2 CFD Model Description

The CFD software used was Fluent (version 6.3.26), which solves the momentum, mass, continuity and energy balance equations for each finite element, in the whole domain of interest. The finite element grid was developed using Gambit (version 2.3.16). Both Gambit and Fluent are developed and commercially distributed by ANSYS, Ltd. Figure 30 shows an image of the model building finite element grid, having near 3 million cells

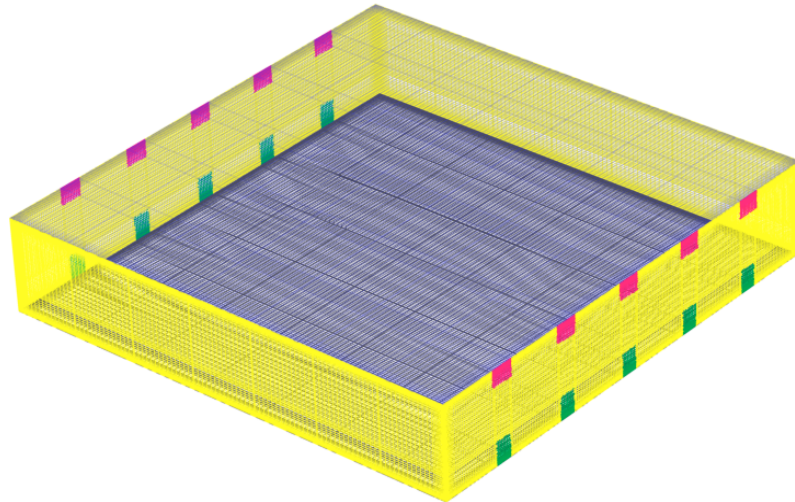


Figure 30 - Image of the building finite element grid

The model has 10 air supply grids near the floor (with 1 m height and 0.75 m width), represented in green, and 10 outflow grids (with 0.75 m height and 1 m width) shown in fuchsia. It also was needed to define the heat sources on the floor. The room has 36 heat sources, designed as small squares (5 cm width), but since they are small, it is not possible to observe them in Figure 30. The walls of the building are colored in yellow and the roof and ceiling in grey. Three possible configurations were studied: a first case where the air was supplied and exhausted on both sides of the room; a second case where the air was supplied and exhausted on the same side of the room; and another case where the air was supplied in just one side but, exhausted on both sides.

The physical models used to solve the equations are listed in .

Table 8 and the boundary conditions used to run the simulation are listed in Table 9.

Table 8 - Physical Models Used

Physical Models and Simulation Conditions	
Density Model	Boussinesq
Radiation Model	Discrete Ordinates
Flow type	Turbulent model: realizable (k-ε) with enhanced wall functions
Unsteady State	

Table 9 - Boundary Conditions used to run the simulation

Location	Boundary Condition	Boundary Condition Description		Units
Walls (N, E, S, W)	Wall	Material	Defined by user	-
		Wall Motion	Stationary	-
		Density	1112	kg/m ³
		Thermal Capacity	1041	J/kg/K
		Thermal Conductivity	0.488	W/m/K
		Shear Condition	No Slip Standard Wall Functions	-
Ceiling	Wall	Material	Defined by user	-
		Wall Motion	Stationary	-
		Density	363	kg/m ³
		Thermal Capacity	960	J/kg/K
		Thermal Conductivity	0.11	W/m/K
		Shear Condition	No Slip Standard Wall Functions	-
Floor	Wall	Material	Defined by user	-
		Wall Motion	Stationary	-
		Density	1061	kg/m ³
		Thermal Capacity	1103	J/kg/K
		Thermal Conductivity	0.52	W/m/K
		Shear Condition	No Slip Standard Wall Functions	-
Supply Grids	Velocity inlet	Velocity, normal to boundary	0.22	m/s
		Temperature	20.5	°C
Exhaust Grids	Outflow	Flow rate weighting	1	-
Interior	Fluid	Material	Air	-
		Viscosity	1.789x10 ⁻⁵	kg/m/s
		Density	Boussinesq	-
		Thermal Capacity	1006.4	J/kg/K

Simulating an unsteady state case, with energy, turbulence and radiation models in a grid with almost 3 million cells requires high computational power, and therefore the simulations were done using the company computer cluster.

3.3.3 EnergyPlus versus Fluent Simulation Results

The results obtained in the CFD simulations were treated using the software TecPlot 360, and will be presented, mostly, in the form of figures with charts and images.

The main objective of this simulation is the comparison with the EP predictions. Due to page limitation, only the results for the first model, with supply and exhaust on both sides, are presented in this thesis.

Figure 31 shows the temperature contours on three planes intercepting the x-axis at 4, 10 and 16 m. Basically, they illustrate the temperature values along the y-axis for each value of z while the planes in Figure 32 illustrate the values along the x-axis for each value of z.

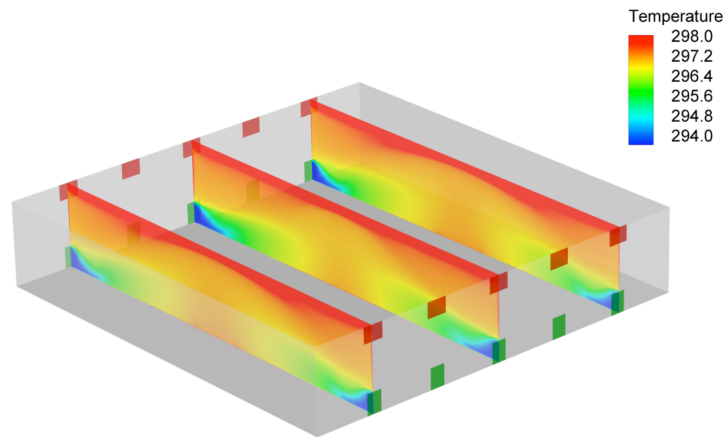


Figure 31 - Temperature contours across the x-axis.

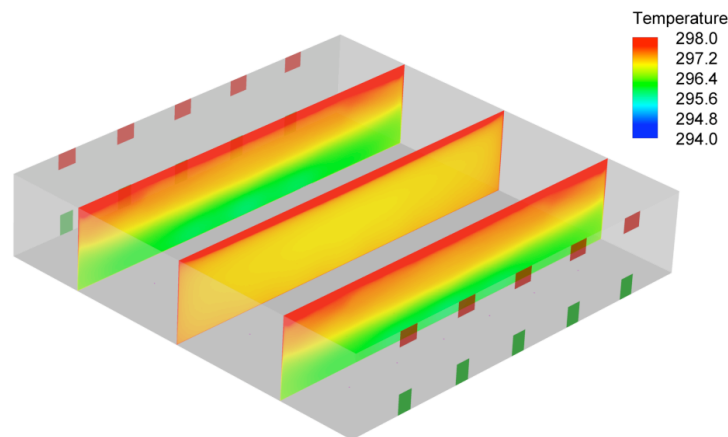


Figure 32 - Temperature contours across the y-axis

It is possible to observe that the room has an obvious stratification. The colder air is near the floor and the warmer is near the ceiling. There is also some warmer air near the walls, resulting from the no slip condition applied. Note that the temperature outside the wall is 29°C and inside the room is between 21 to 25°C. The non-slip condition implies that the layer of fluid near the wall is stagnant and therefore the heat transfer from that layer to the bulk is reduced, resulting in a warmer stagnant layer

Figure 33 shows an iso-temperature surface (24°C), that is, below this surface the temperature is always lower and above is always higher than 24°C.

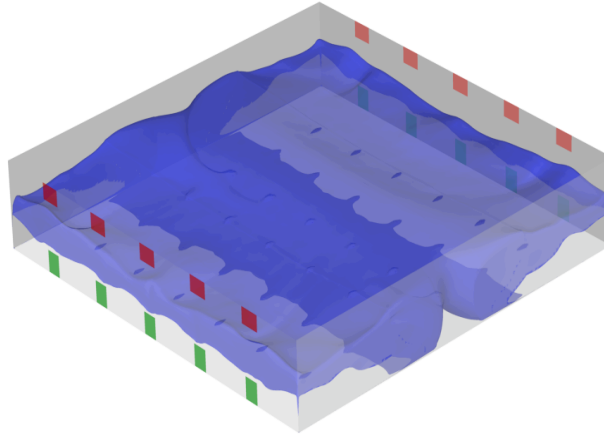


Figure 33 -Iso-temperature surface at 24°C.

The height of this iso-temperature surface is akin to the transition height in EP. Figure 34 shows a histogram with the height distribution for the iso-temperature surface.

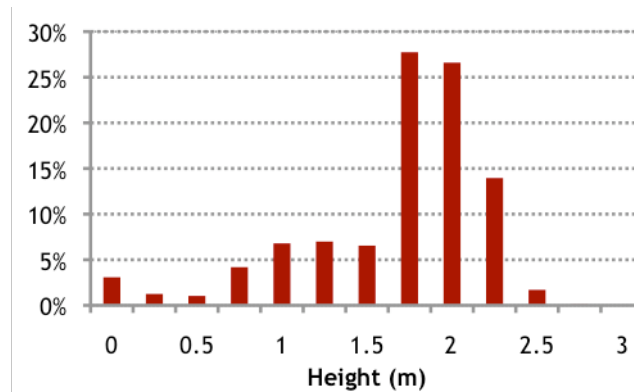


Figure 34 - Height distribution of the iso-temperature surface of Figure 33.

The transition height obtained in EP was 1.7 m. The mean height obtained in the iso-temperature surface is 1.79 m. On the histogram it is possible to note that there are some values below this height, but more than 50% of them lay between 1.75 - 2.25 m. The lower heights are related with the higher temperature in the layer near the walls, and with the influence of the flow in the center of the room. This can be clearly observed by the flow of the air shown with streamlines and temperature contours in Figure 35.

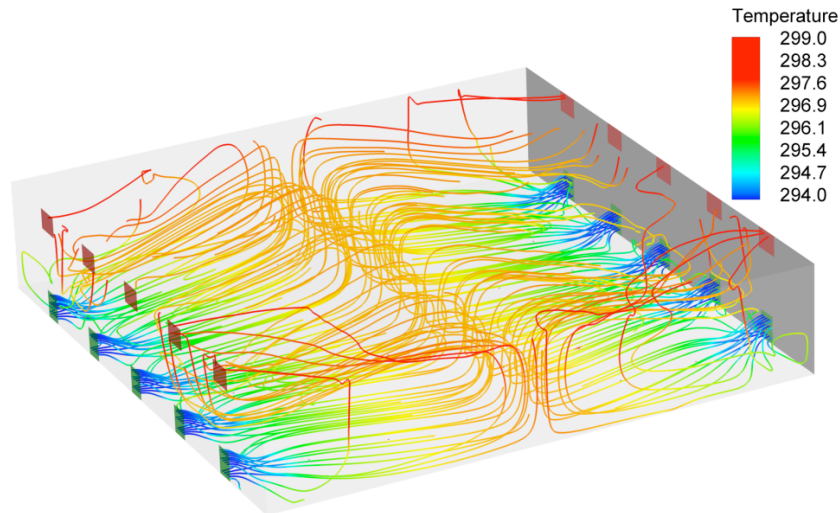


Figure 35 - Streamlines with temperature contours.

Observing Figure 35, it is possible to see that the cold air supplied by the grid, flows near the floor until the center of the room, where it rises as a result of heating and of the flowing air in the opposite direction. It was expected to observe plumes near the heat sources, but this is not possible, because the buoyancy force is not enough to beat the inertia of the flowing air. It is important to note that in CFD the heat transfer depends much on the grid. Usually the boundary layer has only a few millimeters height and in a case like this, it is very difficult to model. A low refinement near the heat sources will result in reduced heat transfer. Unfortunately there was no time to test the influence of the grid refinement near the floor, on the final results.

Figure 36 shows the behavior of the fluid in contact with the heat sources.

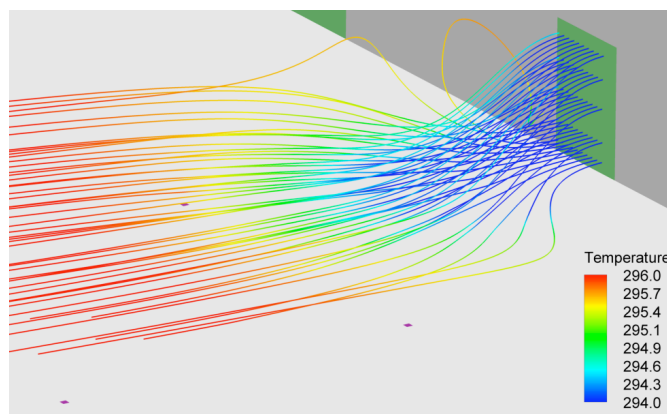


Figure 36 - Detail of the streamlines with temperature contours from the supply inlet grid.

The cold fluid in contact with the heat sources and immediately warms up, but the fluid flow remains unchanged possibly due of the reason stated above.

Figure 37 shows the temperature versus the room height, across the interception of the plane $x = 8.55$ m with the planes $y = 2$ and $y = 4$ m. Figure 38 illustrates the plane

$x = 8.55$ m with temperature contours. The interceptions are represented as black dashed lines.

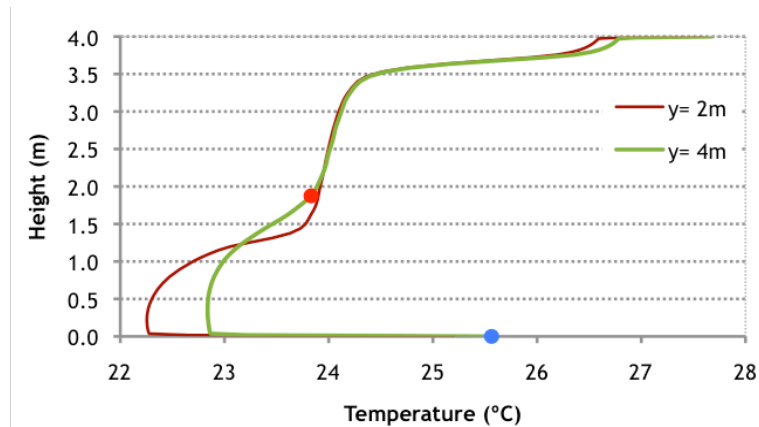


Figure 37 - Height versus temperature for two different y values on plane $x = 8.55$ m (see Figure 38).

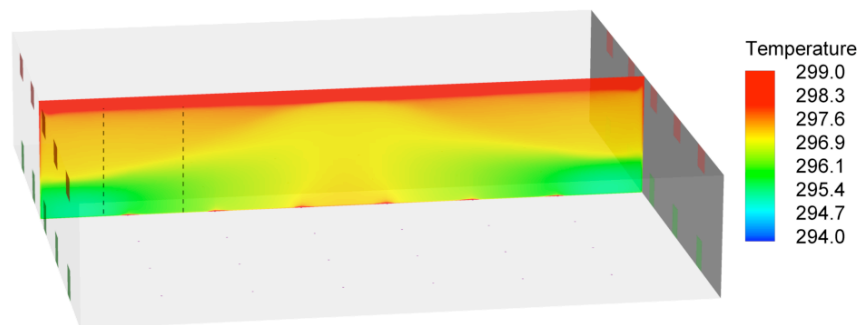


Figure 38 - Temperature contours across the x -axis for $x = 8.55$ m.

Observing Figure 37, it is possible to see both the temperature stratification in the room, and the transition height. The two curves follow the similar trends, the main differences occurring in the temperature up to 1 m in height, which are due the different distances from the air supply grid. Focusing on the green curve, it starts at 25.5°C (blue dot), which is the temperature of the floor slab, and decreases sharply in the very first centimeters as a result of the layer formed, near the floor, by the supplied cold air. The temperature then increases with height until 1.5 - 2 m, meaning that there is temperature stratification in this zone. Above the 2 m, the temperature is nearly constant until 3.5 m, where it starts to increase abruptly. With the exception of this last situation, the results presented on this chart agree with the EP subzone approximation. The zone with lower temperature near the floor is the Floor Subzone in EP, the zone below 1.5 - 2 m is the stratified occupied subzone, and the zone above this is the warmer mixed layer. The abruptly rise of the temperature near the ceiling results from the air accumulation on the top, resulting from the ascending airflow by buoyancy effects and also because of the higher temperature of the ceiling. Note that the red point marks the start of the mixed subzone, meaning that the transition height is about

1.8 m. In Figure 39 it is possible to observe the semblance between the EP and the CFD results

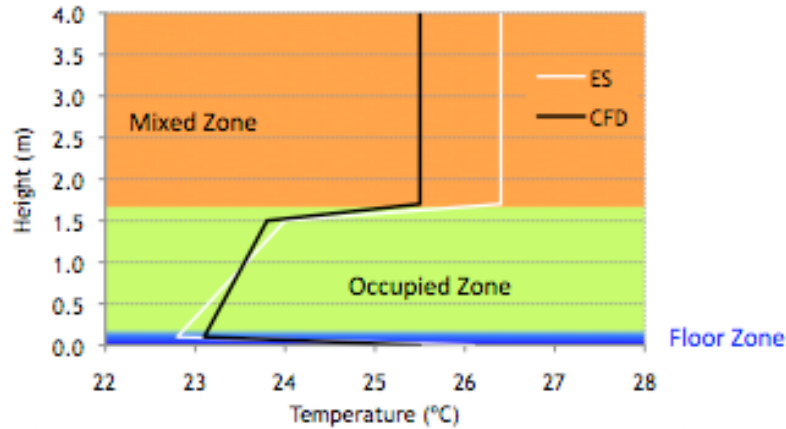


Figure 39 - Temperature profiles inside the room

The prediction of the EP simulations is very close to the CFD results. Table 10 summarizes the average of the most important results from the CFD and EP simulations.

Table 10 - Summary average results from EP and CFD simulations.

Parameter	EnergyPlus	Fluent	Difference (%)
Floor Subzone Temperature	22.8 °C	23.1 °C	1.3
Occupied Subzone Temperature	23.9 °C	23.5 °C	1.7
Mixed Subzone Temperature	26.4 °C	25.5 °C	3.5
Temperature (at TH)	24.0 °C	23.8 °C	0.8
Mean Room Temperature	25.3 °C	24.1 °C	5.1
Transition Height	1.70 m	1.79 m	5.0

The differences listed on Table 10 are between 0.8 to 5.1 %, remaining below the acceptable energy simulation error (10%). It is important to remark that EP had these similar results even without simulating the airflow inside the room, requiring much less computational power and time. It is important to remark that EP considers perfect mixing in the mixed layer, and therefore the 3.5% difference might result from that assumption.

The EP simulations were done in an IBM workstation, consuming about 300 MB RAM and taking 15 minutes to solve. The CFD simulations were done in an IBM computer cluster, requiring 4 processors with 1GB RAM each, and taking 5 days to converge.

3.4 Real Building Model

In this chapter, a study of the DV system performance in an existing building, referred as Building X for reasons of confidentiality is performed. The main subjects of this study are the thermal comfort and the energy consumption. The results will be compared with existing data

of the building consumption and with results obtained with simulation of the actual system implemented.

3.4.1 Model Description

All information used on this model is based on the real operative conditions of the actual building. This information includes: the densities and profiles of occupation; lighting system and equipment; the constructive solutions; and the Air Handling Units nominal power.

3.4.1.1 Geometric model

Building X is an office building located in Lisbon, most precisely in *Parque das Nações*. It has 19 750 m² of serviceable area, distributed throughout 3 underground stories and nine above the ground.

The model was developed in EP, using the GUI *Design Builder* and may be observed in Figure 40, while Figure 41 shows an image of the real building along with the corresponding model image. Both Figures show the level of detail that is possible to obtain with the ES model. Note that in Figure 41, with the exception of the staircase, there are almost no perceptible differences between the model geometry and the real building. In this case the shadowing effects of surrounding buildings were considered, as may be observed in Figure 40.

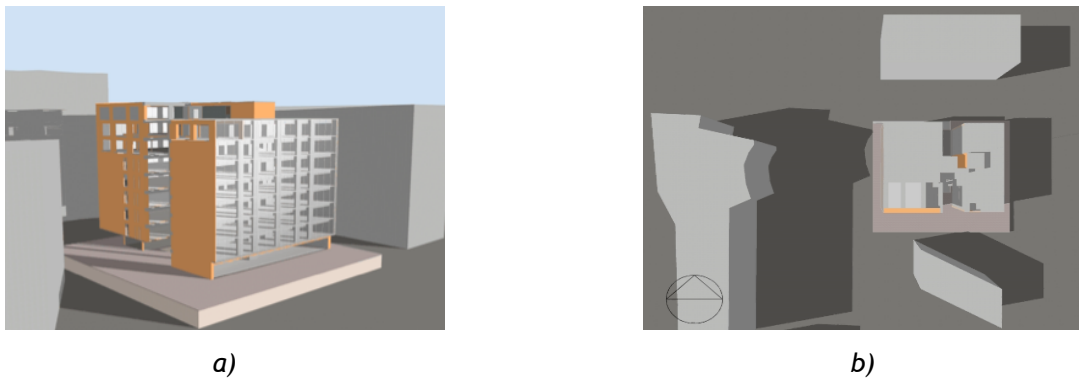


Figure 40 - Images of the model designed using DB and EP. a) Building detail. b) Shadowing effect of building surrounding



Figure 41 - Images of a) the existent building and b) the model used on EP

All the construction materials of the building were considered, in the geometric model. The detailed properties for each constructive solution are presented in APPENDIX B.2.

3.4.1.2 Climate model:

The building is located in Lisbon, which belongs to the summer climatic zone V2 and winter climatic zone I2 (RSECE, 2006).

In the simulation the weather data used was the reference data for Lisbon, existent in the Solterm software, from INETI. The wind speed and direction data used were the existent values on the EP database. Figure 42 to 45 show the characteristic monthly values for that region.

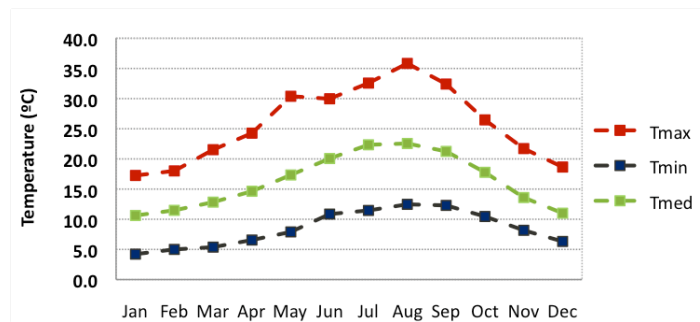


Figure 42 - Monthly maximum, minimum and mean temperatures

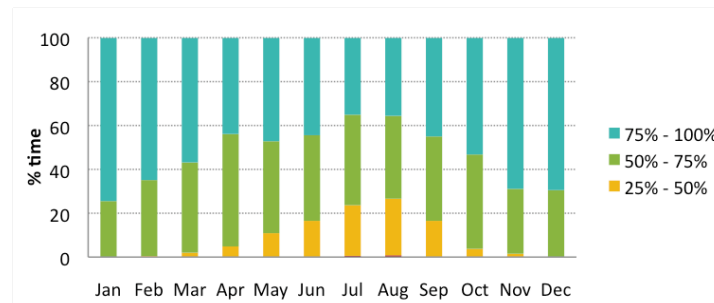
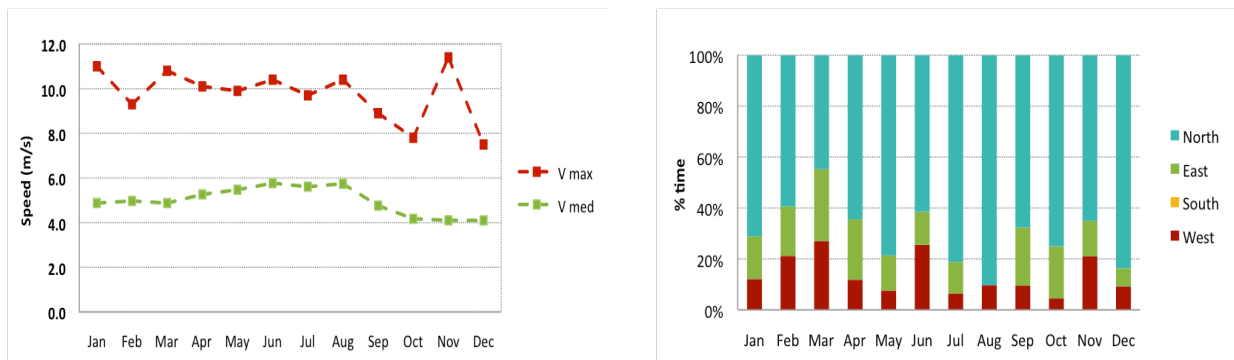


Figure 43 - Monthly time distribution for a given relative humidity



a) b) Figure 44 - Monthly evolution of wind speed (a) and direction (b).

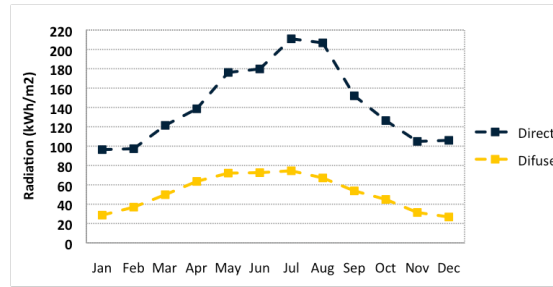


Figure 45 - Total monthly evolution of solar radiation, both diffuse and direct

3.4.1.3 Activity model

Here only a summary of the building operation is given, while the corresponding detailed data, including the profiles of occupation, lighting system and equipment, will be submitted to Appendix B.1. The density of occupation, lighting system and equipment is listed on Table 11.

Table 11 - General densities of occupation, lighting system and equipment

	Density
Occupation	8 m ² /person
Lighting equipment	16 W/m ²
Equipment	5 to 22 W/m ²

People are considered to be writing/sitting, and the heat gains, predicted by ASHRAE, for that activity is 117W/person.

3.4.1.4 Air Conditioning Model

The air conditioning system existing in Building X is a MV system. The system used has the particularity to have induction units in the rooms. In general lines, the principle behind these units, is as follows: the air coming from the air treatment unit, is distributed in the induction units under pressurized, typically 50 to 150 Pa, this will cause the air from the conditioning zone to flow across the cooling/heating coils (from the induction equipment) and mix with the air from the air treatment unit before being supplied, again, to the conditioning zone. Figure 46 illustrates an induction unit operating, during heating and cooling function.



Figure 46 - Induction unit during a) heating and b) cooling operation

3.4.2 Energy Simulation Results

The study of the real building model is focused on the Thermal Comfort and Energy Consumption. The DV system was designed to obtain a transition height of 1.1 m, an acceptable value for office buildings. The set points used on the real building, 23-24°C during the winter and 22-23°C during the summer, were maintained on the MV and DV simulations. Similarly to what was done in the parametric study, both systems were kept as similar as possible. Table 12 resumes the conditions of both systems.

Table 12 - Simulation Conditions for the mixing and displacement ventilation systems

	Mixing Ventilation	Displacement Ventilation
Temperature set point (Summer)	23 - 24°C	
Temperature set point (Winter)	22 - 24°C	
HVAC System Availability	09h - 19h	
Ventilation System	Induction Units	VAV Fan
Outside air controller	No Economizer	Economizer (Free Cooling)

3.4.2.1 Energy Consumption

The energy consumptions predicted in the ES were studied in detail accounting for both the electric and thermal needs. The thermal consumption includes the cooling and heating building demands, while the electric energy consumption is the energy spent in the ventilation units and in the system pumps. Such a detailed study allows predicting where the main energy saving or losses are. One interesting advantage of the DV system over the existing building HVAC system is the possibility of integrating free cooling and for that reason it was applied to the ES Model.

In Figure 47 and 48 it is possible to observe the thermal energy spent, for both systems, during a typical summer and winter period.

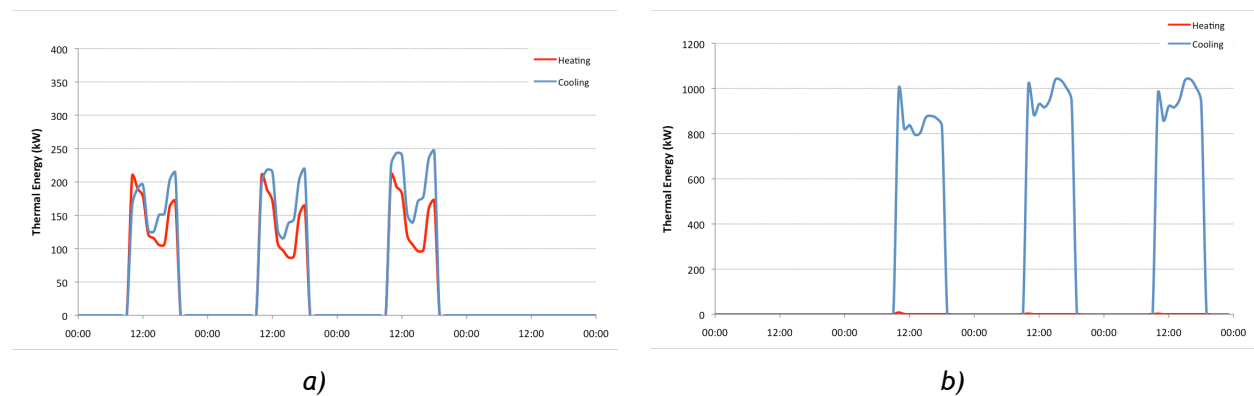


Figure 47 - Thermal energy spent with the current HVAC system, during a typical winter period a) and a typical summer period b)

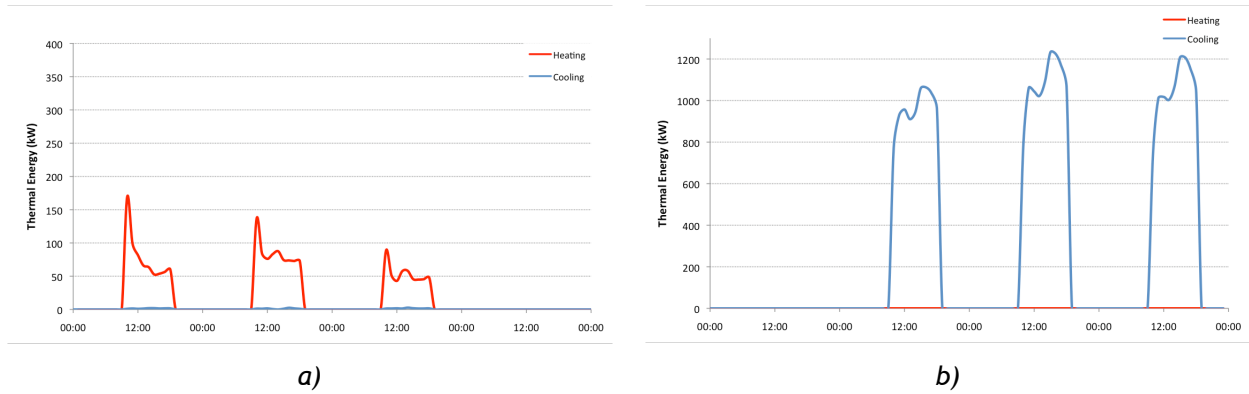


Figure 48 - Thermal energy spent with DV system, during a typical winter period a) and a typical summer period b)

It is possible to observe in Figure 47 that during the winter the building has both cooling and heating energy needs, this fact results from the different needs in each zone, meaning that while there are zones requiring heating, others have cooling needs. Comparing Figure 47 with Figure 48, it is possible to see that the cooling energy spent during winter decreases to almost zero if a DV is used, reflecting the effect of the free-cooling system implemented. The increased cooling energy consumption with DV, during the summer season, results from the increased supply air temperature that will reduce the temperature gradient between the air supply and the room interior.

The monthly energy consumption, for both systems, during the year is presented in Figure 49.

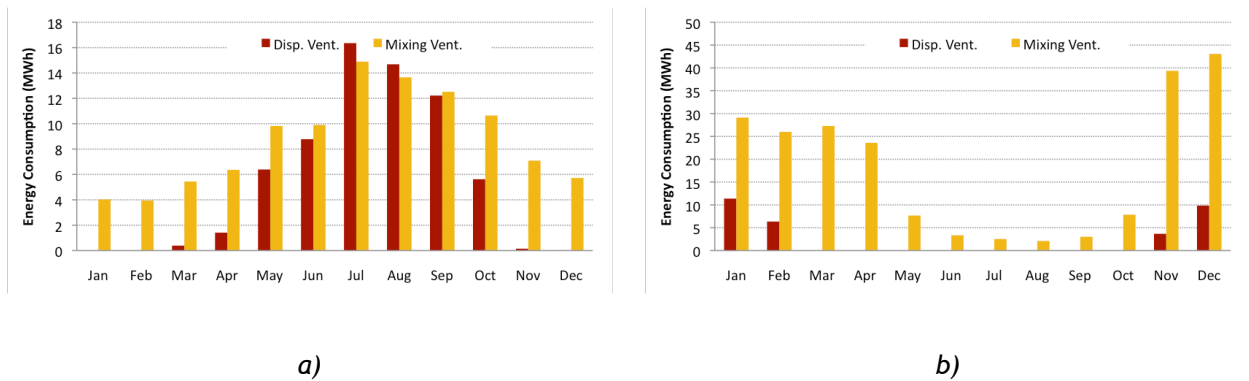


Figure 49 - Monthly energy consumption, for cooling (a) and heating (b), during the year

Observing Figure 49 it is possible to see that when a DV system is used, the thermal energy need is smaller for both heating and cooling. During the heating season, the Cooling energy spent during the colder months is almost reduced to zero, as a consequence of the Free Cooling system used.

As it was explained here, the thermal energy is drastically reduced if a DV system is used. The main advantage of the HVAC system currently operating in Building X is the extremely efficient ventilation. The ventilation through fans for the DV model, is a large disadvantage to the current system since all air is distributed through the use of electric fans.

The lower need of thermal energy in DV system, results in a smaller electric consumption on the chilled and hot water pumps.

Figure 50 summarizes the annual consumption on both systems.

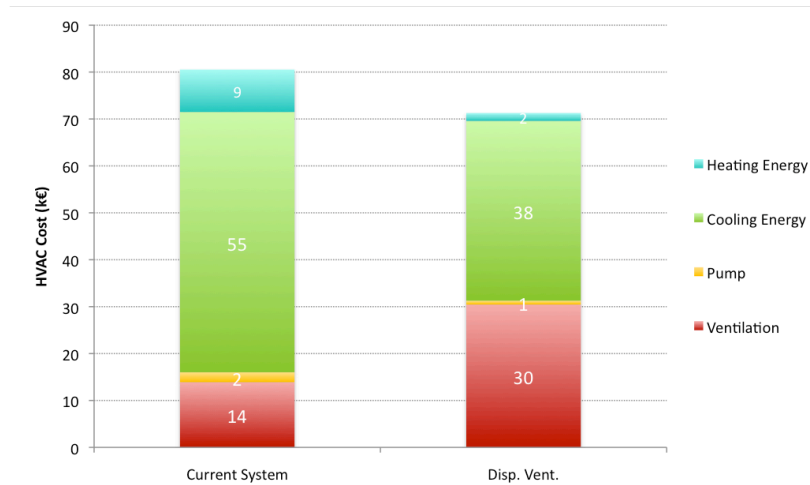


Figure 50 - Summary of the energy spent on both systems

As shown in Figure 50, the energy costs from cooling and heating energy as well as the pump electric energy consumption are smaller when the option is DV. The ventilation energy costs increased with DV option, as a result of the different ventilation system. It is essential to note that if the HVAC system, currently in use at Building X, was a common MV system (ventilated through the use of fans), the ventilation electric energy consumption rise would not be so drastic.

Although there is a much larger consumption in ventilation, the predicted savings resulting from the thermal energy and from the pump consumption are more than enough to balance this difference, resulting in a reduction of 12% of the operational expenses. If the HVAC system was being designed here, it was necessary to balance the initial investment and the operational costs of each system.

As a final note on this topic it is important to say that the operational costs were estimated using the prices of the cooling and heating thermal energy from the cold and hot water network provided by a private company.

3.4.2.2 Thermal Comfort

The comfort of the occupants was also monitored for both systems, and is shown in Figure 51.

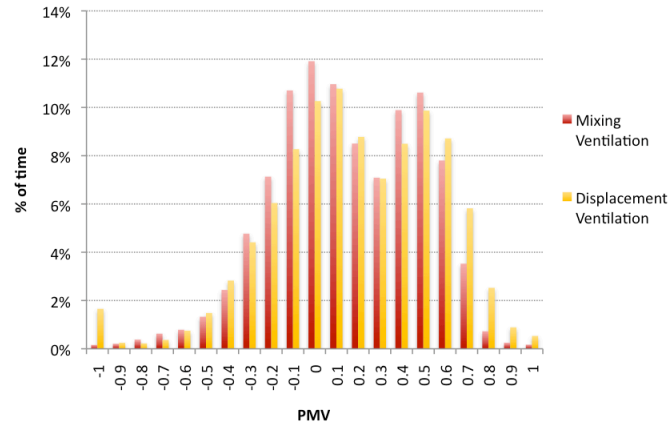


Figure 51 - Predicted mean vote for both systems studied

The comfort conditions are very similar on both cases, but DV is slightly displaced to the right side. Apart from this displacement to the right about 80 % of the time it is within the comfort zone (78 % for DV and 84 % for MV).

It was very important to maintain the comfort conditions in order to have a fair comparison of the operational costs.

As seen in this chapter it was possible to reduce the energy consumption, maintaining the comfort conditions. The savings of 12 % (7900 €/year) obtained with DV, are achieved even with the less efficient ventilation units studied.

It is important to remark that the savings on thermal cooling and heating energy are 31 % (17.2 k€/year) and 81% (7.3 k€/year), respectively.

4 Conclusion

The work presented in this thesis studied the effect of displacement ventilation in energy efficiency and thermal comfort.

The displacement ventilation model, DVAR, existing in the energy simulation software, was studied in detail through a parametric study. The ES model was successfully validated with the comparison of the ES predictions with the Computational Fluid Dynamics results. Differences of less than 5% were obtained, and were considered within the acceptable limit of the ES (10%). It was possible to observe stratification in the room with CFD, validating the ES model assumption. It was not possible to observe plumes rising from the heat sources, a problem that is probably connected with the small size of those sources and with the low refinement of the finite element grid near the floor.

The study developed on the simple building model revealed promising results on the cooling energy savings. It was predicted that the cooling energy on a DV would be reduced to 80% of the thermal energy spent in an equivalent MV system. The comfort conditions were similar on both systems, with 90% of time within the comfort zone. The conditions obtained on DV model were more than acceptable for an office building.

The real building model was built considering the real building information, allowing an enhanced prediction on the energy efficiency and thermal comfort. The energy simulation of the DV system predicted energy savings on the thermal energy consumptions and electric pump consumption while the ventilation electric energy consumption increased. The operational costs resulting from the system modification reduced 12%. The thermal comfort kept almost constant on both systems.

5 Final Remarks

5.1 Accomplished goals

There were many objectives to accomplish in this thesis and, in a general way, all of them were achieved. The comparison between the results of CFD and the prediction of the EP model was done, although some other studies could have been done, as for instance, the betterment of the existent finite element grid or the study of other system condition. However for what it was intended, the objective can be considered achieved.

The implementation in EP of a simple model building, and a real complex building model, was also successfully accomplished. The models included both the DV system and MV system.

The study of the performance of DV system against the mixing ventilation system in a real building was also performed, and their influence in the energy consumption and thermal comfort was studied in depth.

During this work, the author also worked in other projects of the company, mainly related to energy simulation. The projects developed include two hospitals and two office-building towers. The tasks developed for these projects were mostly connected with the development of the buildings models.

It is imperative to state that the training experience received at Fluidinova was crucial in all the achievements of this thesis. The author received intensive formation on Ventilation systems, ES, EP, Design Builder and was also introduced to the CFD software (Gambit 2.3.16, Fluent 6.3.26 and TecPlot 360)

5.2 Future Work

The initial objectives were successfully accomplished. The EP results were validated through comparison with the CFD results; the performance of the DV was studied in a simple office building, as well as in a real office-building tower revealing promising results.

Many interesting work can be developed from here, on both the ES and CFD areas. The Indoor Air Quality can be studied with CFD, using a tracer simulation in the simple room model. The resulting Residence Time Distribution can be then studied as in Chemical Reactor approach.

The other models existing in EP should also be studied in deep and compared with the model used in this thesis.

Finally, it would be very interesting studying the viability of implementation of a DV system in a real building, through an economic balance which should include the initial costs of installation, or modification if the building is already constructed, the operation costs, and the pay back time of the investment.

5.3 Final Appreciations

All the work and studies developed during this thesis were extremely interesting and at the same time it was quite a challenging experience. During this period, many new concepts had to be learned, and the idea of being introduced to a completely new subject was at the a little bit “scary” at beginning, but this subject soon started to converge, to what was learnt at FEUP during my formation as Chemical Engineer. It is gratifying to see that the course learned at that institution is a wide range formation that can be easily adapted to various areas as happened in this case. The possibility of trying what was learnt through the wonderful world of simulation was also very motivating.

It was also an excellent experience to be integrated in a company with such a young and amazing spirit as Fuidinova’s. All the work developed along everything that was learnt and lived there was more than worthwhile.

6 References

Allocca, C. (2001). *Single-sided Natural Ventilation: Design Analysis and General Guidelines*. Massachusetts Institute Of Technology, Department of Mechanical Engineering, Massachusetts.

Arens, A. D. (2000). *Evaluation Of Displacement Ventilation For Use in High-Ceiling Facilities*. MSc Thesis, Massachusetts Institute of Technology, Mechanical Engineering.

ASHRAE. (2005). *Fundamentals*. Atlanta: ASHRAE.

ASHRAE. (2008). *HVAC Systems and Equipment*. Atlanta, USA: ASHRAE.

Butler, D. (2002). *Air conditioning using displacement ventilation to maximize free cooling*. BRE's Environmental Engineering Centre.

Chen, Q. (., & Olsen, E. L. (2002, August 21). Energy consumption and comfort analysis for different low-energy cooling systems in a mild climate. (Elsevier, Ed.) *Energy and Buildings* , 35, pp. 561-571.

Cheong, K., Yua, W., Sekhar, S., Tham, K., & Kosonen, R. (2007, September 07). Local thermal sensation and comfort study in a field environment chamber served by displacement ventilation system in the tropics. *Building and Environment* , 42, pp. 525-533.

Deevy, M., Sinai, Y., Everitt, P., Voigt, L., & Gobeau, N. (2007, February 6). Modelling the effect of an occupant on displacement ventilation with computational fluid dynamics. *Energy and Buildings* , 40, pp. 255-264 .

DOE EnergyPlus. (2005). *EnergyPlus Engineering Reference*. US Department of Energy, California.

DOE EnergyPlus. (2007). *EnergyPlus Input/Output Reference*. US Department Of Energy, California.

Fitzgerald, S. D., & Woods, A. W. (2007). On the transition from displacementto mixing ventilation with a localized heat source. (Elsevier, Ed.) *Building and Environment* , 42, pp. 2210-2217.

Graça, G. C. (2003). *High Performance Commercial Building Systems, Simplified models for heat transfer in rooms*. University of California, San Diego.

Griffith, B. T. (2002). *Incorporating Nodal and Zonal Room Air Models into Building Energy Calculation Procedures* . MSc Thesis, University of California, Mechanical Engineering , Berkley.

Hensen, J. L., Hamelinck, M. J., & Loomans, M. G. *Modelling Approaches for Displacement Ventilation in Offices*. Scotland.

Howell, S., & Potts, I. On the natural displacement flow through a full-scale enclosure, and the importance of the radiative participation of the water vapour content of the ambient air. *Building and Environment* , 37, 817 - 823 .

Hunt, G., & Linden, P. (1999). The fluid mechanics of natural ventilation-displacement ventilation by buoyancy-driven flows assisted by wind. *Building and Environment* , 34, pp. 707-720 .

Lau, J., & Chen, Q. (2007, January 26). Floor-supply displacement ventilation for workshops. *Building and Environment* (42), pp. 1718-1730.

Lin, Z., Chow, T. T., Fong, K. F., Wang, Q., & Li, Y. (2005). Comparison of performances of displacement and mixing ventilations - thermal comfort. *International Journal of Refrigeration* , 28, pp. 276-287.

Lin, Z., Chow, T., Tsang, C., Fong, K., & Chan, L. (2004). CFD study on effect of the air supply location on the performance of the displacement ventilation system. *Building and Environment* .

Müller, D., & Kriegel, M. *Enhanced CFD predictions for displacement ventilation systems*. Technical University of Berlin, Berlin.

Mundt, E. (1996). *The performance of displacement ventilation systems - experimental and theoretical studies*. PhD Thesis, Royal Institute of Technology, Stockholm.

Mundt, E., Skistad, H., Nielsen, P. V., Hagstrom, K., & Railio, J. (2004). *Sistemas De Ventilação Por Deslocamento em Espaços Não Industriais* (Vol. 14). Lisboa: Rehva.

Olsen, E. L. (2002). *Performance Comparison of U.K. Low-Energy Cooling Systems by Energy Simulation*. Massachusetts Institute of Technology , Department of Architecture , Massachusetts.

Skistad, H. (n.d.). *Efficient Ventilation: Displacement Ventilation And Air Curtain Zoning*. Norway.

Song, F., Zhao, B., Yang, X., Jiang, Y., Gopal, V., Dobbs, G., et al. (2008). A new approach on zonal modeling of indoor environment with mechanical ventilation. *Building and Environment* , 43, 278-286.

Sousa, R. G., Madureira, M. F., Gomes, P. J., & Lopes, J. C. (2006) *Utilização de CFD (Computação em Fluidos Dinâmicos) no Projecto de Sistemas de Ventilação*. Fluidinova. Maia: ENVENT.

Száday, E. S. Validation of CFD simulation for displacement ventilation. *I.J. of Simulation*, 6 (downloaded from <http://ducati.doc.ntu.ac.uk/uksim/journal/Vol-6/No.%205/Szaday.pdf> in 20/05/2008)

Yang, T. (2004). *CFD and Field Testing of a Naturally Ventilated Full-scale Building*. PhD Thesis, The University of Nottingham, School of Civil Engineering, Nottingham.

Zhai, Z. (2003). *Developing an Integrated Building Design Tool By Coupling Building Energy Simulation and CFD*. Massachusetts Institute of Technology, Department of Architecture, Massachusetts.

Appendix A. Detailed RSECE Information

In this appendix the detailed information for office building, predicted by RSECE, will be presented.

Figure A.1 to Figure A.3 present the profiles of occupation, lighting system and equipment, respectively.

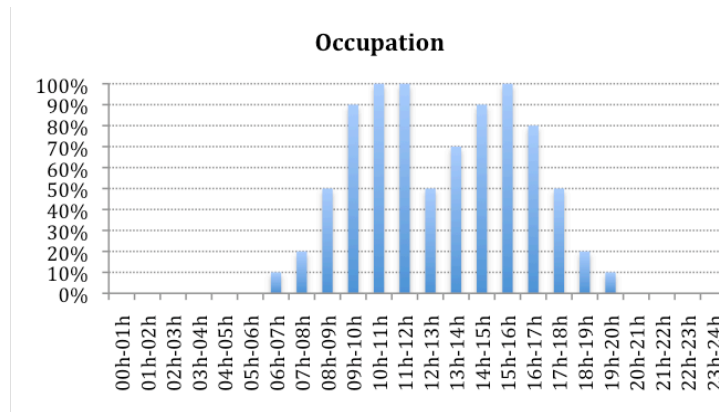


Figure A.1 - Occupation profile, predicted by RSECE

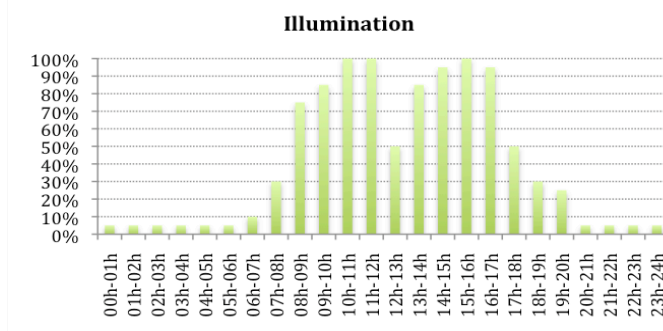


Figure A.2 - Lighting system profile, predicted by RSECE

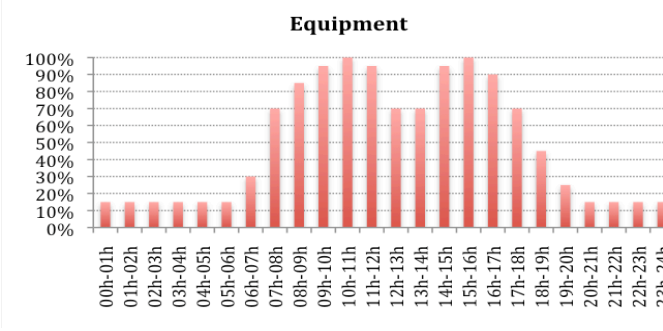


Figure A.3 - Equipment operation profile, predicted by RSECE

The next table lists the densities, predicted by RSECE, for occupation, lighting system and equipment of office buildings.

Table A. 1 - Densities of occupation, lighting system and equipment.

	Densities
Occupation	15 m ² /Occupant
Lighting system	Not defined
Equipment	15 W/m ²

Appendix B. Detailed Information about Real Building (Building X)

In this Appendix detailed information about the real operative conditions is given. This information include the profiles of occupation, lighting system and equipment operation, as well as, their densities.

B.1 Profiles of occupation, lighting system and equipment

Figure B. 1Figure B. 3 illustrate the real activity profiles of Building X

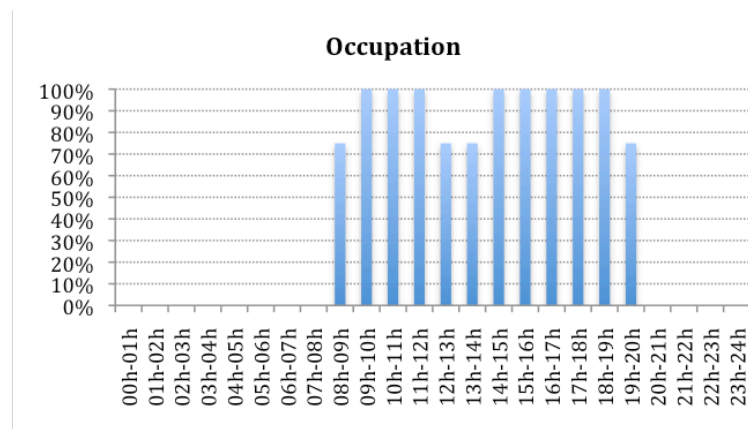


Figure B. 1 - Real building occupation profile

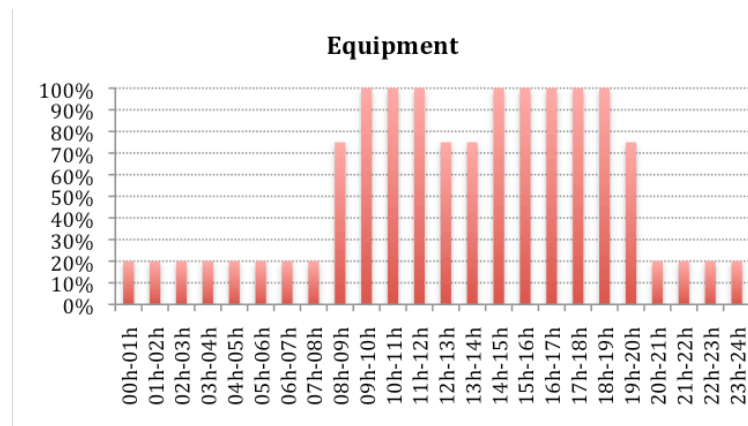


Figure B. 2 - Real building equipment operation profile

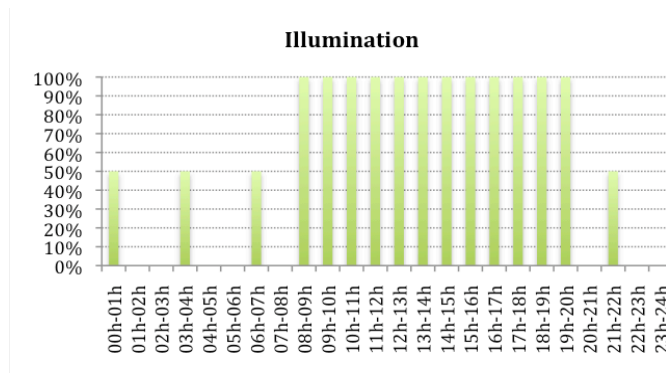


Figure B. 3 - Real building lighting system profile

Table B. 1 lists the densities of lighting system and equipment and Table B. 2 lists the occupation density for each story.

Table B. 1 - Densities of lighting system and equipment

Densities	
Occupation	(See next table)
Lighting system	16 W/m ²
Equipment	5 - 22 W/m ²

Table B. 2 - Density of occupation per story

Story	Occupation
1	20
2	205
3	203
4	169
5	161
6	167
7	152
8	65
9	38

B.2 Constructive Solutions of Building X:

Table B. 4Table B. 10 list all the constructive solutions used in the real building model, including the external walls, internal walls, intermediate slabs, ceiling and Glazing

Table B. 4 - Constructive solution for the external walls of the building

Material	Espessura (m)	U (W/m ² °C)
Reboco laranja	0.020	0.47
Bloco betão	0.200	
Caixa-de-ar	0.020	
Isolamento	0.040	
Bloco betão	0.200	
Gesso cartonado	0.020	

Table B. 4 - Materials used in the interior walls and respective thickness

Material	Espessura (m)
Reboco	0.020
Tijolo furado	0.110
Reboco	0.020

Table B. 5 - Materials used in the intermediate slabs and respective thickness

Material	Espessura (m)
Revestimento vinilico	0.005
Ar	0.060
Camada de forma	0.020
Laje maciça betão	0.180
Caixa-de-ar	0.500
Gesso cartonado	0.020

Table B. 6 - Constructive solution used in the ceiling

Material	Espessura (m)	U (W/m ² °C)
Laje maciça betão	0.180	0.46
Isolamento	0.060	
Camada de forma	0.100	
Caixa-de-ar	0.500	
Gesso cartonado	0.020	

Table B. 7 - Glazing solution applied on the west façade

Fachada Poente			
Propriedades/Vidro	Exterior	Interior	
Espessura (mm)	8.0	10.4	
k (W/m ² /°C)	1.0	1.0	
Factores Energéticos	Transmissão	0.396	0.662
	Reflexão Exterior	0.240	0.064
	Reflexão Interior	0.372	0.064
Factores Luminosos	Transmissão	0.387	0.867
	Reflexão Exterior	0.184	0.078
	Reflexão Interior	0.138	0.078

$$U = 1.7 \text{ W/m}^2/\text{°C}$$

$$\text{Factor Solar} = 0.38$$

$$\text{Transmissão luminosa: } 0.60$$

$$\text{Lâmina de ar: } 12 \text{ mm}$$

Table B. 8 - Glazing solution applied on the east facade

Fachada Nascente			
Propriedades/Vidro	Exterior	Interior	
Espessura (mm)	8.0	10.4	
k (W/m ² /°C)	1.0	1.0	
Factores Energéticos	Transmissão	0.531	0.662
	Reflexão Exterior	0.161	0.064
	Reflexão Interior	0.236	0.064
Factores Luminosos	Transmissão	0.818	0.867
	Reflexão Exterior	0.089	0.078
	Reflexão Interior	0.063	0.078

$$U = 1.7 \text{ W/m}^2/\text{°C}$$

$$\text{Factor Solar} = 0.50$$

$$\text{Transmissão luminosa: } 0.71$$

$$\text{Lâmina de ar: } 12 \text{ mm}$$

Table B. 10 - Glazing solution

applied on the Curtain

Facade

Curtain Facade		
Propriedades/Vidro		Exterior
k (W/m/°C)		5.4
Factores Energéticos	Transmissão	0.303
	Reflexão Exterior	0.050
	Reflexão Interior	0.050
Factores Luminosos	Transmissão	0.640
	Reflexão Exterior	0.063
	Reflexão Interior	0.063

Exterior: 8 mm Parsol Green

Intermédio: 1.52 mm PVB normal

Interior: 8 mm Planilux

Factor Solar: 0.47